



A Thermodynamic Analysis of Solid Oxide Fuel Cells

A Major Qualifying Project submitted to the Faculty of
WORCESTER POLYTECHNIC INSTITUTE
in partial fulfillment of the requirements for the degree of
Bachelor of Science

by:
Mostafa Chehadeh
Tarik Ourdyl
Devan Blechinger-Slocum
Mitra Tabandeh

Date:
April 28th, 2022

Report Submitted to:

Professor Yu Zhong
Worcester Polytechnic Institute

This report represents the work of WPI undergraduate students submitted to the faculty as evidence of a degree requirement. WPI routinely publishes these reports on its website without editorial or peer review. For more information about the project's program at WPI, see <http://www.wpi.edu/Academics/Pro>

Abstract

Fuel cell systems are an emerging engineering technology used to address the energy industry's main approaches to power generation by offering a unique methodology in energy production. A Solid Oxide Fuel Cell (SOFC) is one type of fuel cell system, composed of an anode, cathode, and electrolyte made of solid oxide materials that utilize the reaction between hydrogen fuel and oxygen to generate electricity. In the current study, a heavy-duty cell performance model is modeled using simulation tools to analyze the thermodynamic processes for comparison with experimental observations to guarantee simulation validity. Two robust chemical engineering simulation software packages, i.e., Aspen Plus and IDAES, were employed to investigate the SOFC. The simulations determined the influences of gas compositions, outlet parameters, operating temperature, and inlet fuel pressure on SOFC efficiency. In addition, based on the simulation results, recommendations were made for optimizing the performance of SOFC.

Acknowledgements

Our team would like to acknowledge and thank the individuals and organizations who have made this project possible through their guidance and contributions. We thank Dr. Yu Zhong for supporting and advising us throughout the duration of this project and his willingness to support us through any problems that arose. We would also like to thank Jize Zhang for his assistance in supporting the professor through the proper channels and in our technical writing.. We would also like to thank Saint-Gobain Research North America for their support, as well as Dr. John Pietras from the SGRNA Process Technology Group and Dr. Whitney Colella from the Gaia Energy Research Institute for taking the time to go over our research and provide valuable feedback. Without their support, this project would not be possible.

Executive Summary

Energy manufacturers have been looking for alternative energy production methods that seek the highest standard of efficiency, energy output, and sustainability while reducing their environmental impact. Fuel cells, which are electrochemical devices that can produce electricity by oxidizing fuel through a reversible process, have recently become a strong candidate. Compared to other fuel cell systems developed through the years, Solid Oxide Fuel Cells are arguably the strongest candidate as they provide a list of benefits. SOFCs are highly efficient yet low cost and are favored for their applicability for transportation and stationary power applications. In addition, the reversible process that converts the device into a Solid Oxide Electrolyser cell makes it an excellent option for sustainability.

This report focuses on analyzing the thermodynamic efficiency of SOFCs to make the appropriate recommendations to improve the system. As a result of the fast-advancing field of technology in the digital age, we conducted our analysis through simulation software without the need for physical resources like cell and stack components or fuel.

To ensure a thorough thermodynamic analysis, our team ran two simulations on different softwares: IDAES and Aspen. By comparing the results from different simulations, we aimed to produce accurate conclusions and recommendations.

The IDAES platform uses already existing models for components like compressors, heaters, heat exchangers, and reactors to produce simulation data. Since IDAES uses Python, the platform is also open source, allowing users access to models and Python's wide range of libraries and tools. However, IDAES only allows interaction through text-based programming, making user interaction laborious. The challenging installation process can also stand in the way of initial access.

Aspen is one of the most used chemical process simulation software packages in the chemical and energy industry ("Design and Optimize", n.d.). The platform is user-friendly since it allows for accessible property and process modifications. It also has many features, including equation-oriented modeling and case study features, essential to our SOFC simulation. The pre-existing property values for heterogeneous and homogeneous species reduce the data input necessary to run the simulation. Even so, like IDAES, Aspen has its own limitations. It is primarily up to the user to state assumptions for each simulation. Since Aspen is a chemical

software, electrochemical reactions, vital to the analysis of SOFC, necessitate the incorporation of coding models.

Our simulations included the two vital components of a SOFC stack required for its operation: the electrolyte and its respective electrodes, the anode and cathode. Our model uses a steady-state simulation of a non-reversible SOFC cycle with two main sections. The first is the cycle model, which consists of heat exchangers and heaters. The other section is the SOFC model, consisting of the anode, cathode, and electrolyzer. We further simplified our model by assuming that hydrogen fuel would be utilized, which produces no waste products and utilizes 100% of the fuel. We also assumed all components were perfectly insulated and there was no heat transfer between the components and ambient surroundings. The stack's maximum air temperature and SOFC air outlet temperature were also fixed.

The IDAES software produced a set of graphs over various operating temperatures and constant pressure at 1 atm. These graphs displayed behavior that is typical for SOFC cells. The logarithmic polarization curves plotted together in one graph; all show steep drops at low current densities. When we compare the three polarization curves at various temperatures, we observe a slight increase in cell performance efficiency as operating temperature increases. This increase in our simulation may be lower than expected, likely due to simplified model assumptions. A similar comparison at constant operating temperature and varying pressure shows similar results. As inlet fuel pressure increases, cell performance efficiency increases.

Graphs plotted using data from the Aspen software show similar results, which are also supported by current literature on SOFC efficiency. Graphs show increased performance efficiency with increased operating temperatures. When the current density reaches about 0.6, a rapid decrease in operation begins, as seen in the graphs from both softwares. Additionally, both sets of graphs show the logarithmic curve dip at a current density of around 0.14.

In conclusion, results from the same model simulated on different softwares show similar results, both numerically and in terms of polarization behavior. In addition, increased operating temperatures and fuel inlet pressure improve cell performance efficiency. Other factors that enhance performance are utilizing pure oxygen, higher concentration of hydrogen, and reducing voltage.

Broader Impacts

Engineering Ethics

To employ the principles described in the American Society of Mechanical Engineers (ASME) Code of Ethics of Engineers, we ensured that our knowledge and skills were only used to enhance human welfare. Our team acknowledges that even before we begin our research, we must have a strong understanding of these principles to produce an end result that satisfies all aspects of mechanical engineering.

According to the ASME, the three fundamental principles of their code of ethics are:

1. Using their knowledge and skill for the enhancement of human welfare;
 2. Being honest and impartial, and serving with fidelity their clients (including their employers) and the public;
 3. Striving to increase the competence and prestige of the engineering profession.
- (ASME, 2012)

Throughout this project period, our team's sole objective was to improve fuel cell efficiency to provide low-cost and environmentally friendly stacks for communities around the globe, satisfying the first principle. In addition, throughout our research, simulation, and writing processes, we ensured that all our information was accurate and came from a credible source, which was carefully cited in detail in our references section. Furthermore, by only using accurate and credible data and being honest in our reporting, we were in compliance with the second fundamental principle of ASME's code of ethics. Finally, concerning the third and final principle, we believe that by researching a topic that not only has the power to change the future of energy but is still relatively new in the field of science and engineering, we strive to increase the competence and prestige of the engineering profession.

Societal Impact

SOFCs provide high combined heat and power efficiency and a relatively low cost for an energy source. This allows for stable, long-term clean energy systems in low-income communities. While energy consumption has increased largely due to the growth of many

industries, it remains essential to daily life, even in communities that exist outside the industrial world. Given the state of traditional energy consumption methods and their impact on the environment, it is safe to assume that as global resources start to decrease, certain demographics will suffer the consequences much earlier than others, including low-income communities.

Environmental & Sustainability Impact

Fuel cells are seen as an environmentally friendly alternative to typical fossil fuels corporations would use to produce power since the only byproduct of the SOFC process is water and heat, leading to remarkably reduced pollution and greenhouse gas outputs. In addition, since fuel cells are modular and easy to distribute, there is no need for transmission lines, and they can be easily accessible to remote communities without centralizing an energy system (Stambouli & Traversa, 2002). This would reduce the environmental impact of said transmission lines.

However, some researchers claim hydrogen escapes the system and travels out into the atmosphere. These leftovers would drastically impact the hydrogen cycle and affect the ozone layer. With the hydrogen reaching the stratosphere, it creates more clouds, impacting the polar vortex at both the north and south pole. Holes in the ozone layer would become larger and last even longer. There has not been much research regarding this specific topic. Regardless, we hope that through our research into SOFCs, we can make recommendations that would improve fuel cell systems, which would be beneficial to the environment and our society.

Table of Contents

Abstract	1i
Acknowledgements	2i
Executive Summary	3i
Broader Impacts	5i
Engineering Ethics	5i
Societal Impact	5i
Environmental & Sustainability Impact	6i
Table of Contents	7i
1. Introduction	1
2. Background	2
2.1 Thermal Properties	2
2.1.1 Energy	2
2.1.2 Entropy	2
2.1.3 Exergy	3
2.2 Fuel Cells/SOFCs	3
2.2.1 Mechanical Processes	3
2.2.2 Chemical/Thermodynamic Processes	5
2.2.3 Cell vs Stack	6
2.2.4 Fuel Cell Efficiency	7
2.3 Modeling of Solid Oxide Cells	9
2.3.1 Power Generation Mode	9
2.3.2 Electrolysis Mode	14
2.4 Current Challenges/Limitations	16
2.4.1 Challenges	16
2.4.2 Limitations	16
3. Methodology	17
3.1 IDAES	17
3.1.1 Overview	18
3.1.2 Framework Features	18
3.2 Aspen Plus	20
3.2.1 Overview	20
3.2.2 Framework Features	20
3.3 Simplest SOFC Case	21
3.3.1 SOFC Model	21
	7i

3.3.2 Modeling Assumptions	22
3.3.3 Determination of SOFC Model Constants	22
4. Results and Discussion	24
4.1 IDAES Modeling	24
4.1.1 IDAES Coding	24
4.1.2 Results and Discussion	25
4.2 Aspen Plus Modeling	28
4.2.1 Aspen Coding	29
4.2.2 Results and Discussion	31
4.3 Comparison of Modeling Techniques	33
4.3.1 Benefits of the Software Packages	33
4.3.2 Limitations of the Software Packages	34
5. Conclusions and Recommendation	36
5.1 Conclusions	36
5.2 Recommendations	38
6. References	39
7. Appendices	44
Appendix A	44
Appendix B	45
Appendix C.1	46
Appendix C.4	49
Appendix C.5	50
Appendix C.6	51
Appendix D	52
Appendix E	59
Appendix F	60
Appendix G	61

1. Introduction

Energy consumerism, including coal, natural gas, petroleum, and renewable, has been on the rise since the mid 1970s. The only two recent years where energy production outmatched energy consumption were 2019 and 2020. This has led energy productionists to seek for new alternative methods that increase the efficiency and output of energy creating productions, while still maintaining focus on sustainability. More recently, fuel cells have been perceived as electrochemical devices that do just that. However, these fuel cells are not electrochemical producers, rather they are electrochemical converters. They produce electricity from the oxidation of fuel and the process can be reversible as well. The goal of this project is to analyze a typical Solid Oxide Fuel Cell in the hopes of providing recommendations in areas regarding thermal dynamic efficiency, waste, and output.

However, while Solid Oxide Fuel Cells (SOFCs) are strong and efficient candidates for alternative energy production, the dependence on many operational parameters make it difficult to maximize efficiency and minimize cell degradation. They are additionally difficult to maintain over time, degrading quickly and losing performance.

In order to find ways to accentuate the benefits of SOFCs and minimize their negatives, this project has three main research objectives. The primary objective is to conduct a comprehensive thermodynamic analysis of SOFC stacks using simulation techniques to examine the effects of various operating conditions. To do this, both the Aspen Plus and the IDAES simulation softwares will be used. The other two objectives are to analyze the benefits and limitations of each software.

2. Background

2.1 Thermal Properties

2.1.1 Energy

When analyzing a thermodynamic system, it is essential to evaluate the transfer of energy between the system and its surroundings. Energy in a thermodynamic system is a preserved quantity that describes the state of the system. It must be transferred from one body to another to either provide heat or do work (UWSP, n.d.). Energy is described by the first law of thermodynamics:

$$\Delta U = Q - W$$

where U is the internal energy of the system, Q is heat applied to the system by its surroundings, and W is work done by the system on its surroundings. In a thermodynamic system, all energy is transferred either by heat or by work (Khan Academy, n.d.).

2.1.2 Entropy

The concept of entropy is described by the second law of thermodynamics. It is based on the fact that natural processes can only run in one direction, and entropy is the value that dictates this (Entropy, 2021). Entropy can be described as the log of the total number of different configurations, or states, of a system, using the following equation:

$$\text{Equation 1: } S - S_0 = k_B \ln \Omega$$

where S is entropy, S_0 is the entropy of the system at absolute zero (in most cases, this is zero), k_B is the Boltzmann constant, and Ω is the number of microstates of the system. This means that if a system is at its lowest energy state, the ground state, there is exactly one configuration, which equates to an entropy of zero. As the system increases in energy, more configurations arise, resulting in higher entropy (Entropy, 2022). Essentially, the more disordered a system is, the higher its entropy. The second law also states that entropy can only increase in a closed system. This refers to the fact that heat can only transfer from a region of high temperature to a region of low temperature (Boundless, n.d.). The following equation describes how entropy changes:

$$\text{Equation 2: } dS = \frac{\delta Q}{T}$$

This equation tells us that a small change in entropy occurs when a small amount of heat is transferred to a system by its surroundings, and that entropy change is equal to the change in heat divided by the average temperature of the system and its surroundings.

2.1.3 Exergy

The final, and perhaps most crucial, element of thermodynamic analysis is exergy. This is a measure of the ability for a system to do work. This definition seems similar to that of energy, however there is one crucial difference: exergy is not conserved. Unlike energy, exergy can be destroyed, and cannot be gained unless introduced externally.

The exergy of a system in a given state is given by the following equation:

$$\text{Equation 3: } E = (U - U_0) + p_0(V - V_0) + T_0(S - S_0) + KE + PE$$

where U , V , S , KE , and PE refer to the internal energy, the volume, the entropy, the kinetic energy, and the potential energy of the system at the specified state, respectively. U_0 , V_0 , etc. refer to these properties at the system's dead state. As you can see, this equation is simply a sum of all the forms of energy that can be made into useful work. Thus, exergy is the maximum work that can be extracted from a system (Moran et al., 2014).

2.2 Fuel Cells/SOFCs

Fuel cells have been researched and continuously developed for almost two centuries. Fuel cells are electrochemical devices able to utilize fuel such as gas or coal to generate electricity by converting chemical energy without irreversible oxidation (Rasidi, 2019). Multiple fuel cells with different variations popped up, however, there are only two types of fuel cells that were actually able to be commercialized and brought to the market. These two fuel cells are the Polymer Electrolyte Membrane fuel cell and the Solid Oxide Fuel cell (Energy.gov, n.d.). Due to better applicability for transportation and stationary power applications, this report will be focusing on Solid Oxide Fuel Cells.

2.2.1 Mechanical Processes

Fuel cells are broken up into four functional core parts: The electrolyte, anode, cathode, and interconnects. Electrolytes play a key role in electricity fabrication by aiding in the transport of ions as they help to filter the appropriate ions to pass between the anode and cathode. The electrolytes used for Solid Oxide fuel cells are dense, ceramic compounds of metals such as

Calcium or Zirconium oxides (Solid Oxide Fuel Cells Electrolyte, n.d.). In the case of SOFCs, the electrolyte needs to have the capacity of carrying oxygen ions and have no electronic conduction to reduce the amount of current leakage. The most ideal SOFC electrolyte that many units utilize is the yttria doped zirconia. Yttria-doped zirconia is an outstanding electrolyte as it is a pure ionic conductor. In other words, when the non-reactive electrolyte interacts with both the electrodes, it operates as a pure ionic conductor (Tsfai, 2012). Other electrolytes have been researched such as gadolinium-doped ceria and other zirconia compounds such as scandia-stabilized zirconia. These materials have shown instances of higher conductivity and better stability, at the cost of increased price and availability of the material (Hussain & Yangping, 2020). The other two components that work in tandem to end up with the end product of electricity and water are the cathode and anode. These terms change respectively based on whether the device is an SOFC or an SOEC. In the case of this project, we will be referring to the device as an SOFC. As such, the cathode of an SOFC can also be called an oxygen electrode and the anode of an SOFC is referred to as the hydrogen electrode.

When looking at the anode materials, there should be emphasis on the electrochemical performance and microstructure. By minimizing the polarization losses by addressing the two following properties, a high-performance anode will be created (Sarikaya et al, 2012). Two main factors that are heavily sealed in the fabrication of these cells are to have a large surface area and a prominent porous microstructure (Sarikaya et al, 2012). The electrochemical performance is heavily dependent on the triple phase boundary as the reaction takes place at the point of contact between gas and the oxygen ion conductor. By increasing the surface area of the triple phase boundary, we can maximize the anodic reactions, yielding the largest and most efficient result (Fehribach & O'Hayre, 2009). Porous materials are able to maintain a high electronic conductivity, which leads to the device being more thermally efficient and undergoing more electro-catalytic activity. This helps to facilitate faster gas transportation and reaction within the fuel cell (Energy.gov, n.d.). Engineers and manufacturers have been researching different variations of systems with mix and matching anodes and electrolytes including CGO, YZT, LSCM, and BCYN anode systems. When looking at the hydrogen electrode, we also always have to look at its counterpart, the oxygen electrode.

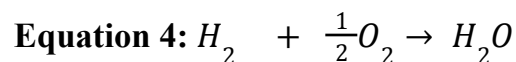
There are multiple mechanical properties that engineers look to when creating and improving SOFCs efficiency. By minimizing the amount of waste from resistance losses, sealing

problems, and other factors, the SOFC thermal efficiency will increase as well (Cerpotech, n.d.) Properties that are great in aiding this effort include high resistance, different geometric choices for components, and utilizing porous supports. Component geometry is a huge aspect in manufacturing processes as it can lead to improvements by incorporating more suitable shapes. In the scenario of SOFCs, tubes are flattened to allow for a higher volume density. This higher density will lead to decreasing the number of sealing problems presented by the SOFC. Porous supports are able to provide better control of the chemical reactions between hydrogen, oxygen, and other gasses. This will improve the efficiency of the SOFC by helping out with the transport of these gasses and heat distribution within the cell (Cerpotech, n.d.).

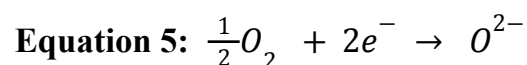
2.2.2 Chemical/Thermodynamic Processes

For the past century, individuals have been trying to learn more about Ohm's law, electrons, conduction, and other aspects regarding electricity. Walter Herman Nerst experimented with different materials to learn more about conduction. He primarily focused on stabilized zirconia, after a breakthrough where he learned that different temperatures affected the electronic and ionic conductivity of the ions. This breakthrough led to the creation of a zirconia filament, used back then as electric light to help illuminate homes. But then, in the 1930s, two scientists named Emil Baur and Hans Preis fabricated a fuel cell concept utilizing zirconium oxide. By incorporating yttria as the electrolyte, the group was able to form the very first SOFC stack (Solid Oxide Fuel Cells, n.d.).

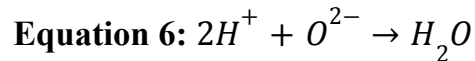
In the individual fuel cells, the electrochemical reaction between oxygen and hydrogen through the catalyst electrode couple, allows the battery to produce current and electricity. It first begins with the oxidation of hydrogen to produce water. This can be characterized by the following redox reaction.



The oxygen is then absorbed onto the other electrode into the cell. This is the direction at which the electrons are flowing. This ionization reaction can be seen below.



Finally, the negatively charged oxygen flows through the electrolyte back to the hydrogen electrode. The hydrogen and oxygen combine to create water.



By placing a solid electrolyte ceramic material between an anode and a cathode, fuel is delivered to the anode and oxidant while air is delivered to the cathode. The electrodes are porous materials that allow both fuel and air to diffuse through. When molecular oxygen is reduced from the cathode side to anode side, fuel diffuses through the anode and interacts with the oxygen ions, releasing electrons and producing electricity. (Solid Oxide Fuel Cells, n.d.)

2.2.3 Cell vs Stack

Individual fuel cells are able to produce electricity, but not to the amounts that stakeholders are seeking for. To help increase the magnitude of electricity produced, SOFCs are constructed in a way that allows them to be linked to other fuel cells in series. By utilizing an interconnect, the cathode of a fuel cell and the anode of another fuel cell within the same stack are conjoined. The interconnect is typically a metallic or ceramic material. There are a few properties that are required for this interconnect to effectively work. The interconnect needs to be resistant to oxidation, chemically stable, and impermeable to the diffusion of gasses put through the SOFC. This leads to an increase in voltage and power to achieve fuel cell requirements mentioned by customers (IOPscience, n.d.). Once a number of stacks have been arrayed, then the whole array becomes a SOFC module. These modules can be integrated into systems to convert the direct current into electricity.

Baur and Preis were the first individuals to succeed in the creation of the first SOFC stack. They originally observed that SOFCs are incredibly powerful tools in the production of electricity and saw the potential in competing with batteries. Despite succeeding, there were a number of flaws and areas where the device could be heavily improved. For example, the resistance was not low enough as manufacturing processes had to reform the electrolyte to be dramatically thinner. The stacking formation and interconnections between the cells had to be improved upon. Lastly, The electrodes and the materials used to create them were sub-par. Overall, there were a number of improvements still to be made and by focusing more on the fuel reactions and system operation, these improvements can eventually be achieved, leading to an improved fuel cell efficiency (Fan et al, 2021).

2.2.4 Fuel Cell Efficiency

The irreversible oxidation and chemical reactions that occur can be interpreted utilizing thermodynamics. When looking at any energy conversion device, efficiency is seen to be one of the greatest properties to try and maximize. In thermodynamic terms, this would refer to the free enthalpy of the reaction of the fuel with the oxidant. The largest issue in improving SOFC's comes from this thermodynamic aspect. More specifically, researchers and engineers are always trying to improve two flaws with an ideal cell, with one being the irreversible mixing of gasses. This mixing leads to a decrease in exergetic quality with voltage drops occurring as more fuel is progressively being used. The other flaw is fuel utilization losses and the ohmic resistance coupled with it. This ohmic resistance generates unnecessary heat for the mechanism (Fuel Cell Fundamentals, n.d.). Both of these flaws lead to the SOFC not utilizing all of the fuel given. Up to 10% of fuel can be found post-process within the fuel stream as it exits the cell (Solid Oxide Fuel Cells, n.d.). More can be learned about the irreversible entropy production of an ohmic loss in a SOFC. By learning how the mixing effects during fuel utilization can be reduced, it will eventually allow for a reversible SOFC operation. Any reactant within the SOFC must have the same thermodynamic state in a reversible cell.

Efficiency is defined as the amount of useful energy that can be extracted from a process relative to the total energy evolved from the process.

$$\text{Equation 7: } \varepsilon = \frac{\text{Useful energy}}{\text{Total Energy}} = \frac{\text{work}}{\Delta \hat{h}}$$

These equations are to calculate the theoretical values for a fuel cell. However, in a real application, this is never truly the case due to a number of factors. As such, the following is a practical equation used to calculate the real efficiency of a fuel cell;

$$\text{Equation 8: } \varepsilon_{real} = (\varepsilon_{thermo}) * (\varepsilon_{Voltage}) * (\varepsilon_{fuel})$$

where (ε_{thermo}) is the reversible thermodynamic efficiency, $(\varepsilon_{Voltage})$ is the voltage efficiency, and (ε_{fuel}) is the fuel utilization efficiency.

Reverse thermodynamic efficiency helps to illustrate that even under ideal conditions, not all the enthalpy contained can be exploited to increase fuel cell efficiency. Looking at voltage efficiency of the fuel cell, it includes losses due to irreversible kinetic effects. This can also be seen as the ratio of the real operating voltage of the fuel cell (V) to the thermodynamically

reversible voltage of the fuel cell (E). This is heavily dependent on the current drawn from the fuel cell. As such, the voltage efficiency will vary depending on the current, with higher currents leading to lower voltage efficiency and vice versa. This establishes fuel cells to perform with the most efficiency at lower loads, much different to other tools industry such as combustion engines. Fuel utilization efficiency relates to the fuel utilized in the electrochemical reactions. It states how the fuel cell will never utilize all 100% of the fuel provided. It may undergo other negligent reactions or simply flow without reacting. As such, the fuel utilization efficiency is the ratio of the fuel used by the cell to generate current against the total fuel provided, seen in the following equation.

$$\text{Equation 9: } \epsilon_{fuel} = \frac{i/nF}{v_{fuel}}$$

Overabundance of fuel is seen as a waste so to combat this, fuel cells typically operate in two conditions: constant-flow-rate condition or constant-stoichiometry.

Constant-flow-rate conditioned fuel cells are supplied a constant amount of fuel regardless of the current density. This is to ensure the fuel cell is not started at max current density but this may lead to significant amounts of fuel to be wasted if the current density is operated at lower conditions. Looking at the other condition, constant-stoichiometry is utilized in fuel cells so that the supply of fuel can be adjusted according to the appropriate current density needed, and just a little bit extra for any load it goes under. For example, a fuel cell that operates in this manner with two times more fuel, is referred to as a fuel cell that is 2 times stoichiometric. The following equation for fuel utilization in a stoichiometric condition is

$$\text{Equation 10: } \epsilon_{fuel} = \frac{1}{\lambda}, \text{ where } \lambda = \frac{(v_{fuel})}{i/nF}$$

Using this equation, we are able to derive a practical efficiency of a real fuel cell by incorporating the aspects of the fuel cell that impact fuel utilization including losses, irreversible kinetic losses, and thermodynamic effects. This equation can be further simplified for fuel cells running in stoichiometric conditions.

$$\text{Equation 11: } \epsilon_{real} = \left(\frac{\hat{\Delta}g}{\hat{\Delta}h_{HHV}} \right) \left(\frac{V}{E} \right) \left(\frac{i/nF}{v_{fuel}} \right)$$

$$\text{Equation 12: } \epsilon_{real} = \left(\frac{\hat{\Delta}g}{\hat{\Delta}h_{HHV}} \right) \left(\frac{V}{E} \right) \left(\frac{1}{\lambda} \right)$$

2.3 Modeling of Solid Oxide Cells

As described above, solid oxide cells have two main modes of operation, the power generation mode and electrolysis mode. Both of these modes contribute to the idea of a reversible solid oxide cell, where one cell is able to operate as both a power generation fuel cell that is able to generate power and an electrolysis cell where it is able to generate fuel. Solid oxide fuel cell and electrolyzer systems are key elements of the energy system's transformation towards sustainability. Solid oxide fuel cells (SOFC) convert fuel to electrical energy with an efficiency of up to 60% and some even higher. Solid oxide electrolyzer cells (SOEC) enable the efficient storage of electrical energy and the production of renewable fuels (Baldi et al., 2019). Solid oxide cells operate at very high temperatures and various advanced ceramic materials are used in their production. The properties and the quality of the ceramic materials strongly influence the performance as well as the durability of the SOFC/SOEC cell and stack. Both solid oxide cells have been modeled by researchers to thermodynamically analyze these cells and use them as hybrids with other electromechanical systems. Examples of these models will be described in the following sections.

2.3.1 Power Generation Mode

The power generation mode of a fuel cell refers to the “Solid Oxide Fuel Cell” portion of the fuel cell, where power/electricity is generated. These high-temperature fuel cells have shown very significant potential for use in power production applications and products. Figure 1 below shows a possible modeling diagram of the SOFC system showing the anode and cathode inputs and outputs. Currently, SOFC systems are the most mature of many options, compared to Solid Oxide Electrolyzer Cell (SOEC) systems. These systems operate in the range of 750-1000C, which makes it possible to combine the SOFC with other conventional thermal cycles to further improve its thermal efficiency (Baldi et al, 2019). This hybrid SOFC system is considered to be key technology in achieving future energy goals, based on the many advantages that it offers over other systems. Having the hybrid SOFC power plant system allows the system to be modeled and thermodynamically analyzed.

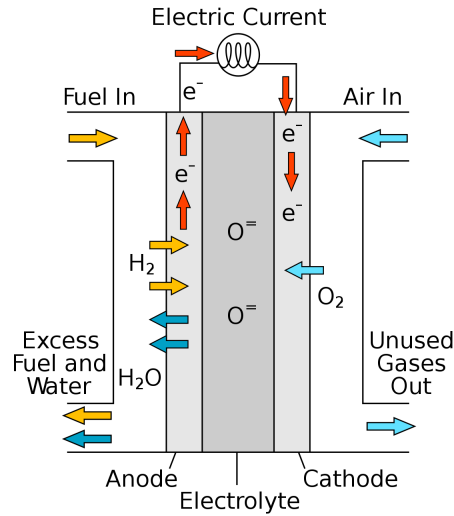


Figure 1: Solid Oxide Fuel Cell (SOFC) model diagram use to represent system (Solid oxide fuel cell, 2022)

A study conducted by Masoud Rokni of the Technical University of Denmark presented a small-scale SOFC-Stirling Engine CHP plant that was thermodynamically analyzed (Rokni, 2013). Modeling and thermodynamically analyzing this hybrid plant can give information regarding other models since this study also focused on the type of natural gas that was used in the system. The findings can be applied to many other hybrid or even reversible systems in order to generate fuel (Rokni, 2013).

The SOFC model developed in Rokni's study was based on the planar-type SOFC and is assumed to be zero-dimensional. For electromechanical modeling, the operation voltage E_{cell} of the fuel cell is calculated as follows where E_{Nernst} , ΔE_{act} , ΔE_{ohm} , ΔE_{conc} , ΔE_{offset} are the Nernst ideal reversible voltage, activation polarization, ohmic polarization, concentration polarization and offset polarization:

$$\mathbf{Equation\ 13:} \quad E_{cell} = E_{Nernst} - \Delta E_{act} - \Delta E_{ohm} - \Delta E_{conc} - \Delta E_{offset}$$

Polarization is generally caused by chemical and physical factors associated with various elements in the fuel cells, such as temperature, pressure, gas composition and fuel properties. These factors limit the reaction processes when the current flows through. The polarization is typically modeled in a polarization curve which displays the voltage output of the fuel cell for a given current density loading. Polarization curve data is usually obtained using a

potentiostat/galvanostat that draws a fixed current from the fuel cell and measures the fuel cell output voltage. An example of a polarization curve can be shown below in Figure 2:

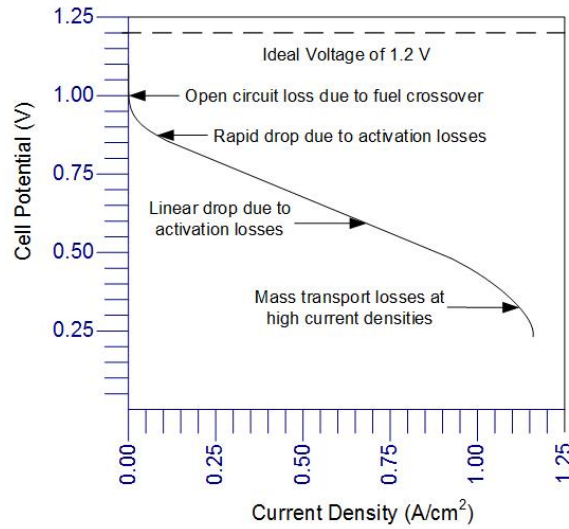


Figure 2: A sample polarization curve of an SOFC system highlighting effect of losses (Spiegel, D. C. (n.d.))

As shown on Figure 2, there are generally three distinct regions of a fuel cell polarization curve. At low power densities, the fuel cell potential decreases due to the activation polarization. At more moderate current densities, the potential decreases linearly due to ohmic losses. At higher current densities, the potential drops further due to concentration polarization. These polarizations are used to calculate the operation voltage of the cell as shown in the equation above. Generally, the ideal voltage value is within a range of 0.9V-1.5V (Lang et al, 2017). This is the voltage value where the current density is equal to 0 A/cm².

Assuming that only hydrogen is electromechanically converted, the Nernst equation can be written as follows:

$$\text{Equation 14: } E_{Nernst} = \frac{-\Delta g_f^0}{\eta_e F} + \frac{RT}{\eta_e F} \ln\left(\frac{P_{H_2, tot} \sqrt{P_{O_2}}}{P_{H_2O}}\right)$$

$$\text{Equation 15: } P_{H_2, tot} = P_{H_2} + P_{CO} + 4P_{CH_4}$$

where Δg_f^0 is the Gibbs free energy at standard pressure, F is the Faraday constant and η_e is the number of charge electrons. R and T are the universal gas constant and the operating temperature.

The Gibbs free energy of the system (the work potential of the fuel) can be calculated as follows:

$$\text{Equation 16: } \Delta g = (-247.4 + 0.0541 * T)$$

This is useful for determining the maximum amount of electrical work that can be extracted from a chemical reaction at a constant pressure and temperature process. Additionally, the spontaneity of a reaction can be determined from the Gibbs free energy. If Δg is equal to zero, then no electrical work can be extracted, if Δg is greater than zero, then work must be input for the reaction to occur, and if Δg is less than zero, then it is energetically favorable and electrical work can be extracted (Fuel Cells & Hydrogen Energy, 2008).

In terms of the Nernst equation above, the Gibbs free energy sets the magnitude of the voltage of the reaction. So if, for example, a reaction has an energy change of -XkJ/mol under standard state conditions, the reversible Nernst voltage will be a net positive value (Fuel Cells & Hydrogen Energy, 2008).

The activation polarization can be calculated using the Butler-Volmer equation to determine the charge transfer coefficients and the exchange current density.

$$\text{Equation 17: } \Delta E_{act} = \frac{RT}{(0.001698T - 1.254)F} \sinh^{-1} \left(\frac{i_d}{2(13.087T - 1.096 * 10^4)} \right)$$

The ohmic polarization depends on the electrical conductivity of the electrodes as well as the ionic conductivity of the electrolyte. It can be calculated as follows where t is the thickness of the anode, electrolyte and cathode, and σ is the conductivity of each respectively:

$$\text{Equation 18: } \Delta E_{ohm} = \left(\frac{t_{an}}{\sigma_{an}} + \frac{t_{el}}{\sigma_{el}} + \frac{t_{ca}}{\sigma_{ca}} \right) i_d$$

The concentration polarization, polarization of an electrolytic cell resulting from changes in the electrolyte concentration, can be calculated by:

$$\text{Equation 19: } \Delta E_{conc} = B \left(- \ln \left(1 + \frac{P_{H2} i_d}{P_{H2O} i_{as}} \right) - \ln \left(1 - \frac{i_d}{i_{as}} \right) \right)$$

where B is the diffusion coefficient, which is equal to

$$\text{Equation 20: } B = (0.008039 X_{H2}^{-1} - 0.007272) \frac{T}{T_{ref}}$$

The anode limiting current, i_{as} , is equal to

$$\text{Equation 21: } i_{as} = \frac{2FP_{H_2} D_{bin} V_{an}}{RT_{an} \tau_{an}}$$

where V_{an} and τ_{an} are the porosity and tortuosity of the anode and

$$\text{Equation 22: } D_{bin} = (-4.107 * 10^{-5} X_{H_2} + 8.704 * 10^{-5}) * \left(\frac{T}{T_{ref}}\right)^{1.75} \frac{p_{ref}}{p}$$

The current density, i_d is equal to

$$\text{Equation 23: } i_d = \frac{\dot{m}_{H_2} 2F}{A}$$

After calculating the operating voltage of the cell, the voltage efficiency of the SOFC cell can be calculated by taking into account the power produced by the SOFC, P_{SOFC} . P_{SOFC} depends on the amount of chemical energy fed to the anode, the reversible efficiency η_{rev} , the voltage efficiency η_v , and the fuel utilization factor U_F . The following equation is used:

$$\text{Equation 24: } P_{SOFC} = (LHV_{H_2} \dot{n}_{H_2,in} + LHV_{CO} \dot{n}_{CO,in} + LHV_{CH_4} \dot{n}_{CH_4,in}) \eta_{rev} \eta_v U_F$$

where U_F is a set value and η_v is defined as

$$\text{Equation 25: } \eta_v = \frac{\Delta E_{cell}}{E_{Nernst}}$$

The reversible efficiency η_{rev} is the maximum possible efficiency that is defined as the relationship between the change in the Gibbs free energy and the fuel's lower heating value as shown in the equation below:

$$\text{Equation 26: } \eta_{rev} = \frac{(\Delta \bar{g}_f)_{fuel}}{LHV_{fuel}}$$

Additionally, the equations for the conservation of mass, energy and momentum were incorporated into Rokni's model. The equations described above are used to conduct the thermodynamic analysis of the SOFC portion of the SOFC-Stirling Engine hybrid. In Rokni's model, a novel hybrid SOFC-Stirling plant with a power capacity of about 10kW was designed and then presented along with the thermodynamic calculations. This type of analysis can be applied to multiple SOFC applications and potentially be used for reversible applications as well as electrolyzer cells. This study serves as an example of how researchers are able to thermodynamically analyze and model Solid Oxide Cells, specifically fuel cells that are in the

power generation mode. For this report, a simpler set-up of an SOFC system will be analyzed (Rokni, 2013).

2.3.2 Electrolysis Mode

The electrolysis mode of the solid oxide cell typically refers to the Solid Oxide Electrolyzer Cell that operates in the reversed manner of an SOFC. SOECs are solid oxide cells that produce fuel, generally hydrogen, from water using electricity. Similar to the SOFC, SOECs operate at very high temperatures (around 800C) and have an efficiency of around 53%. While SOFCs are more widely analyzed, researchers have begun thermodynamically analyzing SOECs by using 2D models and even hydrogen leak estimation (Nafees & Abdul Rasid, 2019). An interesting scenario of SOEC use is storing energy in hydrogen form when renewable power sources do not match the load. So, it is important to study the changing behavior of SOEC systems to know their ability to adapt to the changing power profiles.

A study from the Institut de Robòtica in Barcelona, Spain by researcher A. Cifuentes and others that models an SOEC thermodynamically to quantify the follow of hydrogen that is hypothesized to leak out caused by high temperatures. Their system is modeled in three parts: fluid dynamics, electrochemistry and heat transfer. From this study, the most important part is the electrochemistry part that can be used in other thermodynamic analyses (Cifuentes et al, n.d.).

Similar to the SOFC analysis, the operation voltage of the SOEC stack, V_{cell} can be calculated from the sum of the Nernst voltage, activation voltage (or polarization), ohmic voltage and the concentration voltage as shown below:

$$\text{Equation 27: } V_{cell} = V_{Nernst} + V_{act} + V_{ohm} + V_{conc}$$

This is opposite to what was done for SOFCs where the voltage of the cell was the Nernst voltage minus the sum of the voltage contribution from polarization. This is due to the fact that the SOEC operates in the reverse manner to the SOFC where it consumes electricity to produce fuel.

V_{Nernst} can be calculated as follows:

$$\text{Equation 28: } V_{Nernst} = \frac{\Delta G}{\eta F} + \frac{R T}{\eta F} \ln\left(\frac{P_{H_2} \sqrt{P_{O_2}}}{P_{H_2O}}\right)$$

where ΔG is the increase in Gibbs free energy, η is the number of electron moles transferred in the reaction, R and T are the universal gas constant and cell temperature, F is the Faraday constant, and P is the partial pressure.

The activation voltage V_{act} is calculated as:

$$\text{Equation 29: } V_{act} = \sum_i \frac{R_g T}{\eta F} \sinh^{-1} \left(\frac{J}{2\gamma_i e^{\left(\frac{E_{act,i}}{-R_g T}\right)}} \right)$$

where J is the current density applied to the cell.

The ohmic voltage is calculated as:

$$\text{Equation 30: } V_{ohm} = J * k_{\Omega}$$

where k_{Ω} is the ohmic resistance.

The concentration voltage is divided into the anode and the cathode side contributions:

$$\text{Equation 31: } V_{con} = \frac{R_g T}{nF} \ln \left(\frac{1 + \frac{JR_g T \delta_c}{2FD_{H_2O}^{eff} P_{H_2}}}{1 - \frac{JR_g T \delta_c}{2FD_{H_2O}^{eff} P_{H_2O}}} \right) + \frac{R_g T}{nF} \ln \left(\sqrt{1 + \frac{JR_g T \delta_a}{4FD_{O_2}^{eff} P_{O_2}}} \right)$$

where $D_{H_2O}^{eff}$ and $D_{O_2}^{eff}$ are the effective steam and oxygen diffusion, δ_c is the cathode thickness and δ_a is the anode thickness.

With this analysis, the study then goes into the heat transfer with an energy balance equation to calculate the temperature of the stack. Then to estimate the hydrogen leakage, the heat of the combusted hydrogen is assumed by multiplying the mass flow of the hydrogen leakage by the hydrogen Lower Heating Value (Cifuentes et al, n.d.).

This thermodynamic analysis is an example of how researchers are able to thermodynamically analyze SOEC systems that can be applied to other applications and further develop SOEC systems. Since the SOEC was invented much later than the SOFC, there are many limitations, challenges, and uncertainties that still exist with SOEC systems that are currently being researched compared to the SOFC. In the next sections, the specific limitations and challenges that exist in SOFC and SOEC systems will be discussed.

2.4 Current Challenges/Limitations

There are challenges and limitations concerning the design, materials, cost, efficiency, operation and production process of SOFC systems. In this section we have defined challenges as current difficulties regarding SOFC systems that are expected to be addressed whereas limitations are quantitative factors that determine conditions of operations.

2.4.1 Challenges

According to the United States Department of Energy's report to congress on the status of their SOFC program, there are currently five main goals regarding the improvement of the cells. In the coming years, the Department of Energy aims to increase overall cell efficiency to 60% without carbon capture and sequestration. They are also working on achieving a lifetime of over 40,000 hours and a less than 0.2% per 1,000 hours degradation rate, as well as decreasing the stack cost to less than \$225/kW and the entire system cost to less than \$900/kW. Another challenge SOFC improvement poses is the high operating temperatures (800-1000 °C).

2.4.2 Limitations

One of the main limitations of SOFC's is the ideal operating temperature. SOFC's are at peak fuel efficiency at 1000 °C. A 10% drop in temperature causes an increase in the internal resistance to the flow of oxygen ions, and can result in a 12% drop in overall efficiency (Stambouli & Traversa, 2002). The high operating temperature requires proper thermal insulation for safety, as well as retaining generated heat, which calls for expensive high temperature alloys and ceramics to encase and connect the cell system, increasing the overall cost. Lowering the operating temperature for SOFC's would not only make them cheaper, but reduce thermal stress, improving the life cycle of the whole system. Currently, overlooking efficiency, the lowest temperature a SOFC can function at is 550 °C.

3. Methodology

The following chapters of this report will provide a thermodynamic analysis of SOFC's through the elements of energy, entropy, and exergy. In thermodynamic systems, energy is transferred between bodies by heat or work. As the overall system energy is increased, entropy increases, resulting in the transfer of heat from a high temperature region to a low temperature one in a closed system. The ability of this system to work is defined as exergy, which is not conserved and can only increase if gained externally.

Walter Herman Nernst's idea to use a zirconia filament used previously as electric light, combined with Emil Baur and Hans Preis' fuel cell concept that used zirconium oxide led to the first SOFC stack, utilizing yttria as the electrolyte. Out of all fuel cell concepts that have been researched and developed over the past twenty years, SOFC's have proven to allow for better applicability for transportation and stationary power applications. Their efficiency, low cost, applicability, and sustainability are among the reasons why it is a new and developing technology worth our attention.

In the hopes of aiming to diagram the chemical reactions that occur within the Solid Oxide Fuel Cell, our group compared and contrasted different simulation softwares. The two programs that we looked at were the Institute for the Design of Advanced Energy Systems (IDAES) simulation software and Aspen Simulation Software. Both simulation softwares were explored for modeling SOFCs in order to compare results and provide recommendations to SOFC scientists and researchers on the benefits of each modeling package.

3.1 IDAES



Figure 3: IDAES Logo (*IDAES* (n.d.))

3.1.1 Overview

IDAES, which stands for the Institute of Design of Advanced Energy Systems, is a next-generation, multi-scale modeling and optimization framework used to support the US Energy and Power Industry. It is a powerful and versatile computational platform based in Python that offers next-generation capabilities utilized for complex system and engineering processes. Released in 2020, *IDAES* is built to enable large scale mathematical optimization, concept design, steady-state and dynamic modeling. It also includes automated development of thermodynamic, physical property and kinetic sub-models from experimental data. This allows for modeling of conceptual system designs, power plant design, process operations dynamics, chemical reaction modeling, and more. A platform like *IDAES* can provide the team with reliable simulation data through the use of already existing models for common components such as compressors, heaters, heat exchangers, and reactors. For SOFCs, these property packages will be beneficial for setting up a model that can simulate results (*IDAES*, n.d.).

3.1.2 Framework Features

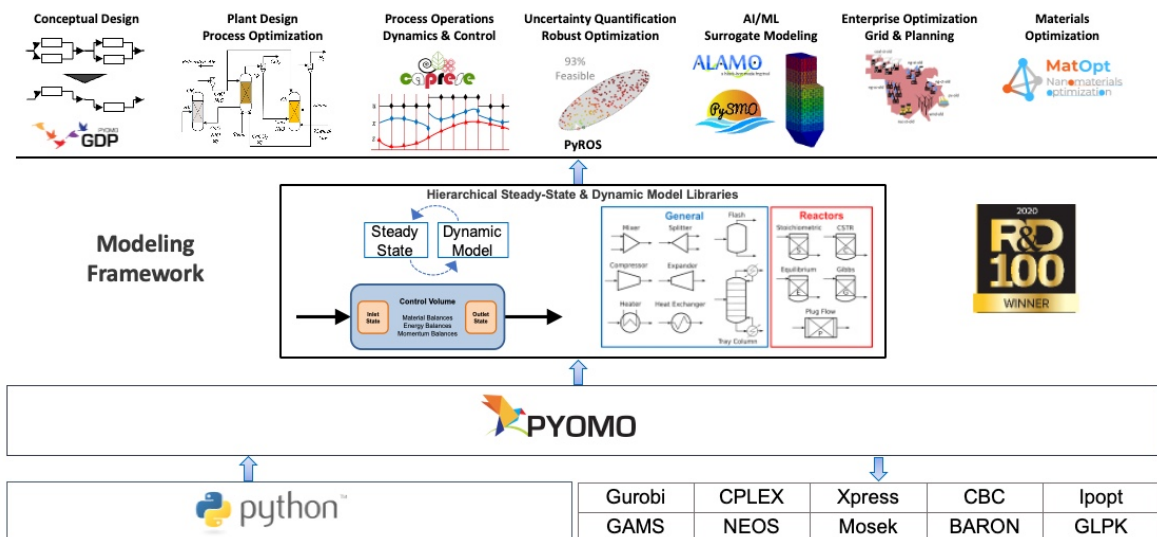


Figure 4: IDAES Platform Flowchart (*IDAES* (n.d.).)

Since *IDAES* is based in Python, a high-level general-purpose programming language, the platform is open source, so any researcher is able to download *IDAES* and utilize its features to model designs. Figure 4 above shows the flowchart in which *IDAES* operates from the lowest Python level to the various applications it can be used to model and supplement. With Python, users get access to Python’s wide range of libraries and tools to use in the *IDAES* environment. The platform is equation oriented, so users can obtain access to a large range of derivative-based

numerical solvers for various problems with support for both linear and nonlinear systems of ordinary and partial differential equations. It is also extensible, so the source code for all the models and tools are open and visible to users. This allows for both seeing and understanding what is happening in any model and being able to easily modify and extend existing models for any researcher's needs.

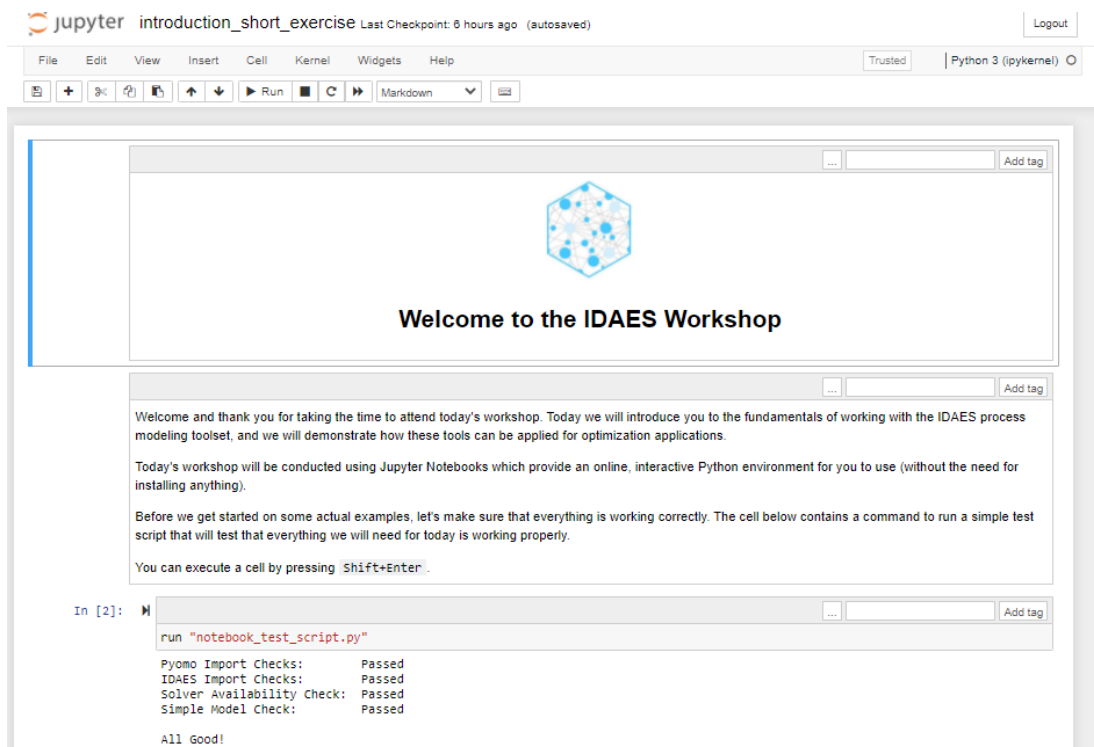


Figure 5: Jupyter Notebooks User Interface from Tutorial Exercises

With its advanced and flexible form, *IDAES* has a large library of property packages, “parameter estimation, model predictive control, uncertainty quantification, and surrogate modeling”. The interface for *IDAES* is done using a web application called *Jupyter Notebooks*. *Jupyter Notebooks* is used for typing and creating the code for the models consisting of blocks of code and text, as shown in Figure 5 above. This gives the user control on which parts of the code they want to run along with text for explaining each block. *Jupyter Notebooks* is generally used for big data integration and has interactive outputs such as graphs, tables, diagrams and flowsheets. Using this platform with its extensive features will provide the team a way to model, simulate and thermodynamically analyze SOFCs. For installation instructions, see Appendix F.

3.2 Aspen Plus

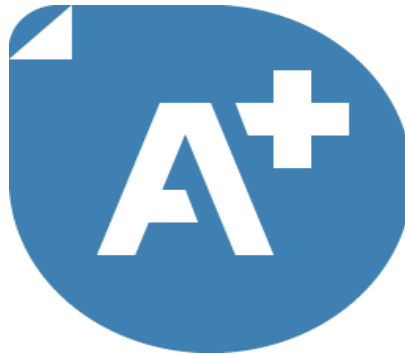


Figure 6: Aspen Plus Logo (*Design and Optimize Chemical Processes with Aspen Plus.* (n.d.))

3.2.1 Overview

ASPEN is the leading chemical process simulation software package that is widely used in different aspects of the industry including chemical and energy fields. ASPEN is a strong software as it can handle very rigorous and complex processes that revolve around chemical reactions, compounds, systems, and even electrolyte solutions, and simulate interactions by utilizing complex calculations such as models, equations, math calculations, and regressions. This is incredibly important in our study of a Solid Oxide Fuel Cell as it allows us to produce outputs with a given process design and thermodynamic inputs. It features rigorous modeling for streams and processing unit operations, making it extremely effective in modeling processes that involve two states of matter, both fluids and solids (AspenTech, n.d.).

3.2.2 Framework Features

The model proposed in this study is intended for the use of steady-state simulation of a non-reversible SOFC cycle. This contains two main sections, with one being the cycle model, which includes the heat exchangers and heaters utilized, and then the SOFC model, which consists of the anode, cathode, and electrolyzer. This would act as the simulation model for the application to run. There are a number of commands and blocks that are used to actually get the simulation to run. This includes defining the flowsheet, inputting global information for calculations, specifying components, entering physical property parameters and data, specific unit operation blocks, and eventually creating plots.

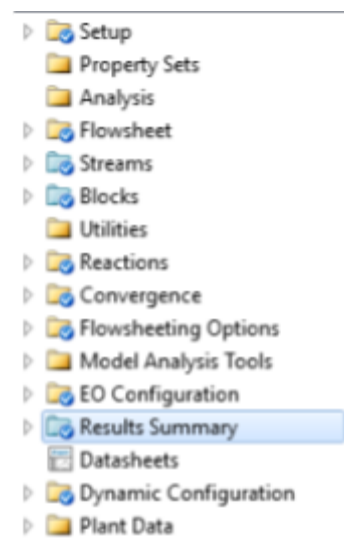


Figure 7: AspenPlus Features

All of these frameworks are important in forming a simulation that is fully controlled and allows for us to optimize the process as well. Since ASPEN is a very user-friendly and driven simulation software, it allows for easy property and process modifications. Other features include equation-oriented modeling, comprehensive unit operations, Thermophysical properties, sensitivity and convergence analysis, and case study features. The latter is the most applicable feature for our project as it allows for the side-by-side comparison of each case study run. This would tackle the problem of trying to determine where areas of the SOFC can be improved and optimized.

3.3 Simplest SOFC Case

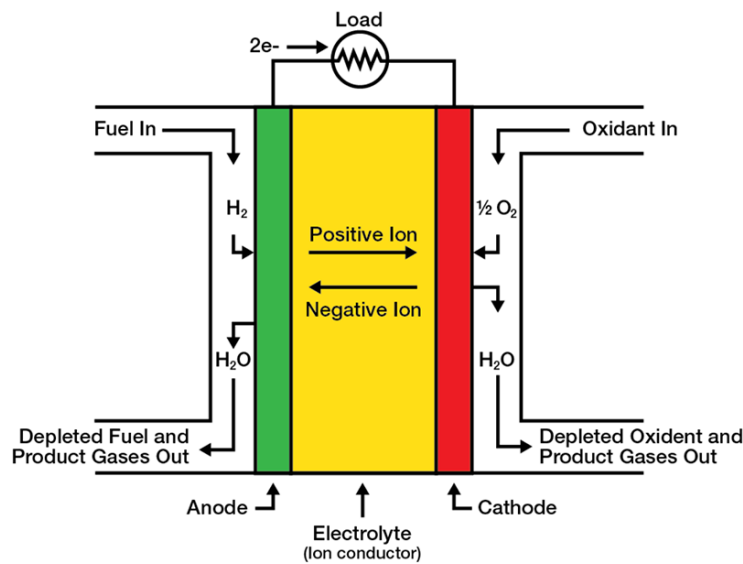


Figure 8: Diagram of a Simple SOFC Model (*SOFC Operating Principle*, (n.d.))

3.3.1 SOFC Model

A number of different components and parts may be used to power an SOFC, however, many of these only help to improve the thermodynamic efficiency of the SOFC. In regards to this project, only three vital parts of the stack are required to ensure proper operation of the SOFC. This includes the electrolyte, electrode, and any of the interconnects between the components. This is considered to be the most simple model of a Solid Oxide Fuel cell. The air flow input is led through the cathode to pass over oxygen ions to the opposite side. On the opposite side, the fuel flow input leads through the anode and retrieves the oxygen ions being transported through the movement of electrons in the electrolyte and the electric current.

3.3.2 Modeling Assumptions

Some assumptions of the thermodynamic model need to be claimed. Assumptions of this thermodynamic model are as stated (Kosaksri et al, n.d.):

- Components are perfectly thermally insulated. Material insulation properties don't allow for the heat transfer between the ambient environment.
- The fuel supplied to the SOFC system is pure Hydrogen [H_2]
- The output of the fuel cell is pure water (all of the hydrogen reacts and forms water)
- SOFC stacks are fabricated as planar fuel cells. These include ceramic cells with metallic interconnects
- Maximum air temperature through a stack is fixed. This is due to the relationship between airflow temperature and cell temperature gradients.
- Current density remains constant through the cell.
- Maximum SOFC air outlet temperature is fixed.
- For a 5"x5"x5" SOFC stack, cell dimensions would be roughly .16"x.16"x.16" (L x W x H)

There are a number of other assumptions that can be included within his report, however, as this case study focuses on the most simple SOFC case, no added components and their assumptions will be included.

3.3.3 Determination of SOFC Model Constants

The model of an energy system consisting of a fuel cell that was developed in this report utilized a set of modeling constants which were supplied as inputs to the codes of the *IDAES* and *Aspen* softwares. These constants were obtained and determined from various literature that supported our assumptions regarding the simple SOFC setup. Table 1 lists the constant values and assumptions that were used in both the *IDAES* and *Aspen* models. Many of the constants such as the concentration coefficients and activation energies were obtained from the same reports to remain consistent with the relationship of these values. These values included constants such as the universal gas constant, Faraday constant and other factors and coefficients. While these values may be appropriate to use for simulating results, it is not certain how well the results obtained using these constants in the SOFC model would match the performance of an actual SOFC due to the lack of physical experimental data in the report.

Table 1: Assumed Constant Values used in the SOFC *IDAES* and *Aspen* Models

Constant	Symbol	Value	Units
Universal Gas Constant	R	8.314	J/K mol
Faraday Constant	F	96485.000	C/mol
Reference Pressure	P_ref	1.000	atm
Limiting Current Density	i_L	0.650	A/cm ²
Limintating Current Density Correction Factor	a	0.050	-
Transfer Coefficient	B	0.500	-
Pre-exponential Factor: Anode	gam_a	20000.000	A/cm ²
Pre-exponential Factor: Cathode	gam_c	15000.000	A/cm ²
Activation Energy: Anode	e_a	105000.000	J/mol
Activation Energy: Cathode	e_c	110000.000	J/mol

In addition to the constant parameters described above, Table 2 below shows a list of the controlled input values that were varied in order to obtain simulated data using both of the software frameworks. The SOFC Operating Temperature (T) was observed in the range of 800-1000C (1073-1273K) as these are general operating temperatures for SOFC systems. The fuel utilization value remained at 1 as we had assumed that all of the hydrogen fuel flowing into the SOFC system was converted into water, thus 100% fuel utilization. The anolyte and catholyte pressures were controlled in order to observe the impact of pressure on the system. Since we assumed 100% fuel utilization and air flowing through the catholyte, the pressure across the anolyte remained constant and the pressure of the catholyte was 21% of the atmospheric pressure. The SOFC resistance value was able to be both calculated or assumed, and this effect was observed for analyzing the impact of SOFC resistance. Various combinations of these values were used for finding parameters that maximize the SOFC efficiency using realistic values.

Table 2: Table of SOFC model controlled input parameters

Input	Symbol	Value	Units
SOFC Operating Temp	T	1273.00	K
Fuel Utilization	fuelU	1.00	
Input Anolyte Pressure	H2_p	1.00	atm
Output Anolyte Pressure	H2O_p	1.00	atm
Catholyte Pressure	O2_p	0.21	atm
SOFC Resistance	R_ohm	0.50	ohm*cm ²

4. Results and Discussion

4.1 IDAES Modeling

The first software used for modeling the simple SOFC system described in Section 3.31 was the IDAES modeling package. As described, IDAES is a Python-based software package that allows the creation of simple and complex models for a variety of problems and processes. The following sections outline the coding used and the results obtained from the coded model.

4.1.1 IDAES Coding

To create a model of a basic SOFC using IDAES, sample code provided by the creators of the program was used as a starting point. This sample modeled an SOFC using natural gas fuel, which is methane. We intended to model an SOFC using pure hydrogen fuel, which simplified the process. We were able to eliminate many extraneous equations by making assumptions as a result of using hydrogen over methane. For example, we were able to assume fuel utilization was 100% since using hydrogen produces no waste products. This simplified many of the required equations.

After adjusting the model to fit our needs, we began calculating the open-circuit voltage of the cell using the Nernst equation:

$$\text{Equation 32: } V_{Nernst} = \frac{\Delta G}{\eta F} + \frac{R_g T}{\eta F} \ln\left(\frac{P_{H_2} \sqrt{P_{O_2}}}{P_{H_2O}}\right)$$

This was fairly straightforward, as we used simple math operations to calculate the voltage. From here, we began generating the polarization curve of the cell.

The polarization curve was generated by calculating values in arrays. We began with an array of current densities, starting from 0.1 A/cm² and going to 0.5 A/cm² in increments of 0.02. From there we calculated the ohmic loss, concentration loss, and activation loss for each current density. Finally, by subtracting these losses from the calculated Nernst voltage, we were able to find the actual voltage produced by the cell for a range of current densities. By plotting the array of current densities on a graph on the x-axis, and the corresponding actual voltages on the y-axis, we were able to generate a polarization curve for the cell (Spiegel, n.d.).

After creating the polarization curve, the total power and overall efficiency of the cell at different current densities were calculated, again by manipulating arrays. This allowed finding the setting with the most power and efficiency. We repeated this entire process for the operating

temperatures of 1273 K, 1173K, 1073K, and 473 K, in order to find optimal parameters for our fuel cell.

As the software is based in Python, the model was hand coded in *Jupyter Notebooks* with knowledge from Python equation-oriented calculations. The code used for the simulations is outlined in Appendix E. This code was imputed into the blocks in *Jupyter Notebooks* and run independently to obtain the graphs and tables following the calculations outlined in literature. These calculations are used to find the voltage of the cell at various current densities ranging from $0.1\text{A}/\text{cm}^2$ to $0.69\text{A}/\text{cm}^2$. This will allow for a large range of data to be collected and plotted so that polarization curves may be obtained for the various input operating conditions.

Standard mathematical coding techniques were used as shown in the coding to first calculate the Nernst voltage. This takes into consideration the input operating temperature and the Gibbs free energy to calculate the Gibbs Energy Change which is then added to the Nernst term relating the input pressures. This gives the Nernst Voltage term. Then the current density is set as a range of values from $0.1\text{A}/\text{cm}^2$ to $0.69\text{A}/\text{cm}^2$ and used to calculate the Ohmic loss for each current density. This is similarly done for the Activation and Concentration losses at each of the current densities. Then the losses and voltages at each current density are summed to get the voltage of the SOFC at each current density. These values are plotted to get the polarization curve of the SOFC for various input operating conditions. Additionally, to verify the OCV (Open Circuit Voltage) of the SOFC, logarithmic polarization curves are plotted for small current densities from $0.0001\text{A}/\text{cm}^2$ to $0.1\text{A}/\text{cm}^2$ on a logarithmic scale.

4.1.2 Results and Discussion

After running the code described in section 4.1.1, the IDAES framework is able to output datasets for the total actual voltage of the simplified SOFC system. This voltage change is plotted over the change in current density of the SOFC system, which will provide a plot of the polarization curve at various input conditions. The datasets examined were for constant pressure conditions at various temperatures and constant temperature conditions at various temperatures. This allows for the analysis on the impact of temperature or pressure on the system thus providing information regarding their effects on the performance of the SOFC system. The efficiency at a default current density of $0.3\text{A}/\text{cm}^2$ of each input condition was plotted over the

pressure and temperature to observe the behavior of the efficiency as the operating temperature and inlet fuel pressure change.

For the initial dataset, the constant pressure conditions for the system were observed and analyzed at a temperature range of 800C (1073K) to 1000C (1273K). This temperature range is typical for high performing SOFC systems. Generally, at higher temperatures, SOFC systems become suitable candidates for applications with heat engine energy recovery devices which increase overall efficiency. At the range of operating temperatures, the pressure of the inlet fuel was set at a constant 1 atm, and since the simplified system has a fuel utilization of 1, the pressure of the outlet water was also 1 atm. The resistance of the SOFC system was set to a constant 0.5 ohm*cm³. Inputting these values outputs simulated graphs shown in Figure 9. All of the graphs display typical behavior of an SOFC system where the voltage of the SOFC decreases as a function of current density and becomes limited at the limiting current density value.

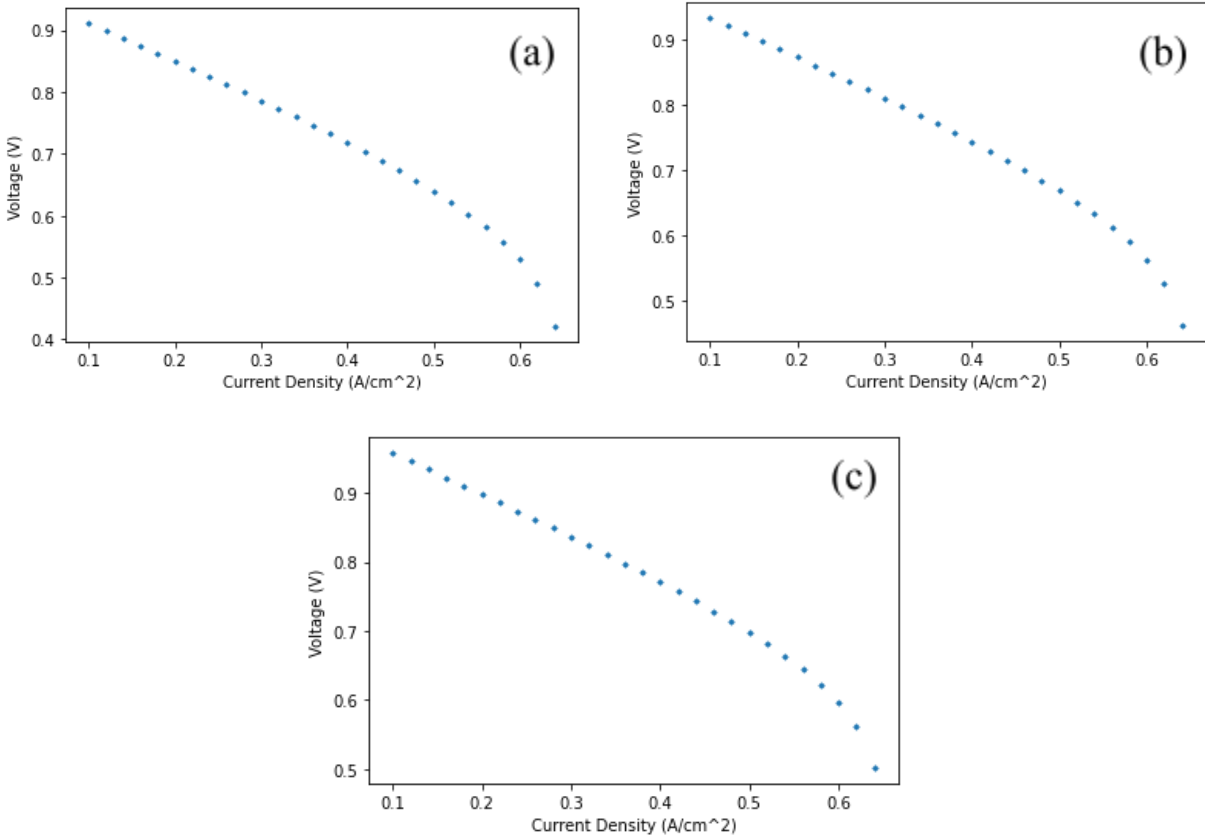


Figure 9: SOFC Simulated Polarization Curves at Various Temperatures (a) 800C, (b) 900C, and (c) 1000C) and Constant Pressure (1 atm)

The plots were then overlaid over each other so that the polarization curve can be compared at the various temperatures. Additionally, logarithmic polarization curves were plotted, shown in Figure 10, in order to observe the effects at very low current densities. This will confirm the Open Circuit Voltage (OCV) value corresponds with the Reversible voltage (E_{rev}) and observe any steep drops of voltage at low current densities. When plotted at each of the various temperatures, the logarithmic curves show evidence of steep drops of voltage at low current densities. For all three graphs, the voltage starts at the calculated OCV value which needs to be in the range of 0.9-1.5V preferably at 1.1V.

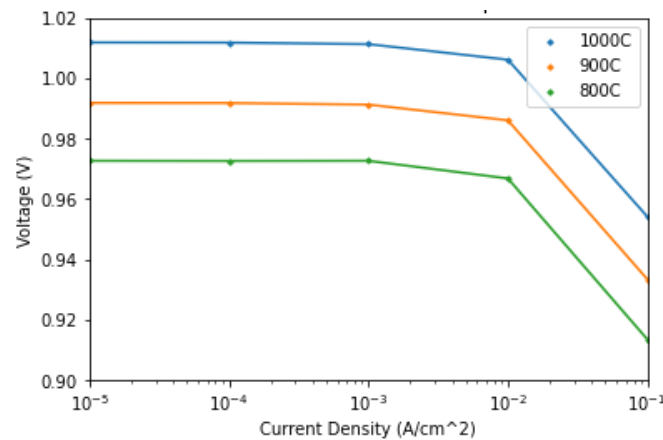


Figure 10: Logarithmic Polarization Curve for Low Current Densities at Various Temperature

From Figure 11a below, the overall curve shifts upward as the operating temperature increases. This represents the overall efficiency performance trend of the system as the operating temperature varies. This matches with current literature and discussions that show that the efficiency should increase as the operating temperature increases. However, there was only a slight increase of the SOFC efficiency as the temperature increased. This may have been due to the simplified model assumptions where the input fuel was completely reacted in the system to produce water and that the inlet fuel pressure is equal to the outlet water pressure. The corresponding efficiency curve shown in Figure 11b also shows that the performance of the system decreases as the operating temperature increases.

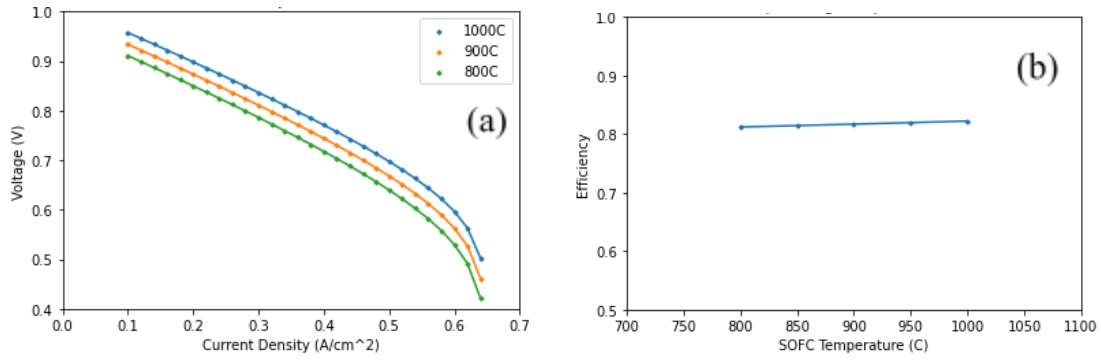


Figure 11: Graphs of the (a) Comparison of the SOFC Polarization Curves at each temperature and (b) the effect of SOFC Operating Temperature on Efficiency

A similar analysis was done for the effects of constant temperature on the SOFC system where the pressure was varied in each simulation. A range of 0.5-3atm of the inlet fuel pressure, and thus the outlet water pressure, was observed at a constant SOFC operating temperature of 1000C (1273K). Generally, higher SOFC inlet fuel pressures yield better performance for the system. From the simulated data, this aspect is shown in the overlaid Figure 12a where the overall polarization curve shifts upward as the inlet fuel pressure increases. Similar to the effect on operating temperature, the shift of the curve refers to the performance of the SOFC system. Corresponding with literature data, the efficiency of the system increases as the inlet fuel pressure increases, which is shown in Figure 12b.

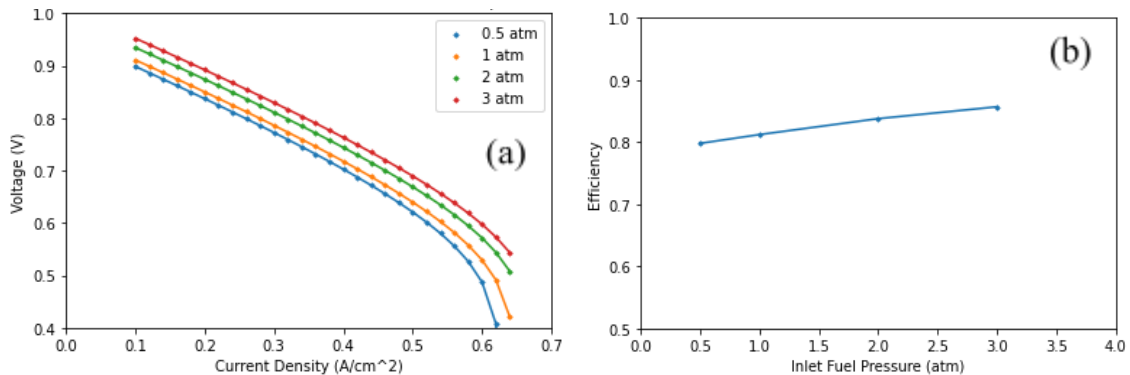


Figure 12: (a) SOFC Polarization Curve at Various Inlet Fuel pressures (0.5-3 atm) and Constant Operation Temperature (1000K) and (b) Graph of the Effect of Inlet Fuel Pressure on the Efficiency of the SOFC

4.2 Aspen Plus Modeling

The second software used for modeling the simple SOFC system was the Aspen Plus modeling simulation package. As described, Aspen is a mathematical model chemical

processes simulator to help with energy costs, equipment design, and process modeling. The following sections outline the flowsheets and the results obtained from the model.

4.2.1 Aspen Coding

Aspen's SOFC simulation began with first drafting a flowsheet that represents the fuels within a system and its flows. There can be multiple inlet fuels but based on the components of the system, only a set number of outlet fuels are allowed, primarily one or two. To simulate the anode, cathode, and electrolyte, a combination of varying heat exchangers were utilized to represent the SOFC. Starting with the cathode, oxygen (A3 Flow) is processed through a heater. Heaters were used as opposed to heat exchangers for the purpose of determining thermal and phase conditions. A4 flow is then used for the input in a separator. A separator is utilized as in a traditional SOFC, air would be used. In this project's scenario, pure oxygen and hydrogen is utilized so separation is not required. After separation, the oxygen (O2-CAT) flows out from the cathode and progresses into the anode. The other flow from the separator (A5-A4-O) represents the unused gas. Since fuel utilization is 1.0, there are no unused gasses left and output is 0. However, a heater was utilized again to illustrate that unused oxygen gas would be implemented back into the system with a higher starting temperature, allowing for minimal waste production (Hauck et al, 2017).

While the oxygen (O2-AN) from the cathode enters the anode, a new input fuel (F6) is put into the system. This goes through a heater and then through a RGibbs Equilibrium reactor. This type of component is utilized in chemical and phase equilibrium by using Gibbs energy minimization or maximizing entropy. For this instance, we do not want to measure the entropy in this scenario but look at the state of the system as a function of pressure and temperature. This reactor also acts as a conversion reactor to convert base components into the necessary products. In this instance, by utilizing the chemical equations previously mentioned in the background, the oxygen input flow from the cathode and the hydrogen input are combined and converted into water. In scenarios where the SOFC is reversible, a second heater is utilized in the anode to heat the water up to begin the electrolysis process. Looking at Figure 14, the flowsheet from Aspen plus depicts the flow direction and components used within the SOFC process.

Aspen Plus offers the ability to provide the chemical and thermodynamic properties of all flow inputs and outputs based on the substance used within the model. In this scenario, it is either hydrogen and oxygen that eventually becomes water. A number of stream properties were

looked at including temperature, pressure, enthalpy, entropy, Gibbs energy, mass and mole flow, internal energy, density, and other properties that were looked at in our research. After completing the flowsheet and the necessary inputs required, the simulation was run. After running the simulation, the results block produced a long list of variables and their values for every point in the system with specific flows. Many of these properties and their values can be found in Appendix D.

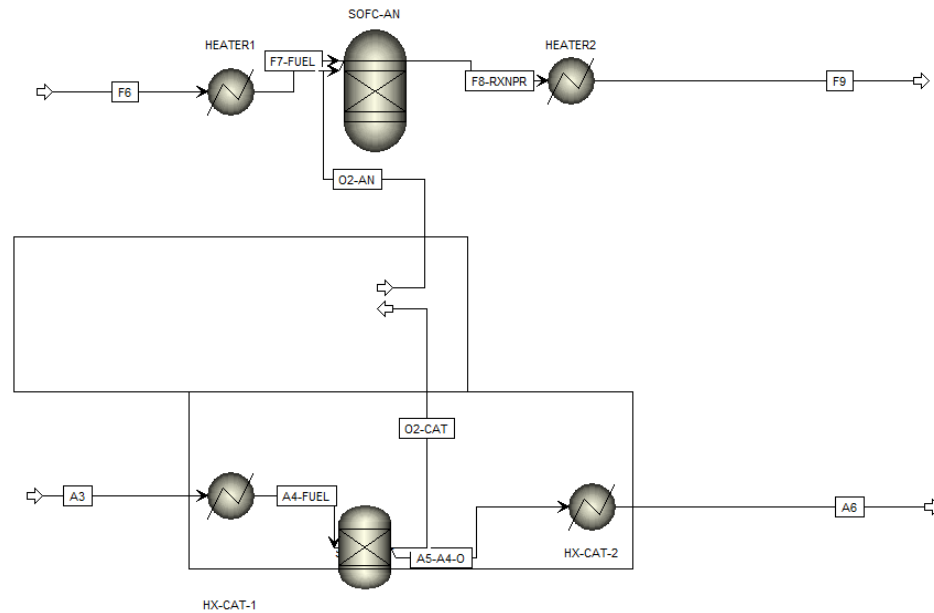


Figure 14: Aspen Plus SOFC Flowsheet

Aspen excelled in obtaining purely chemical results, but when looking at SOFCs, multiple electrochemical properties are looked at, voltage loss being the most notable. Aspen alone can not calculate this, so calculator blocks were utilized to serve as the calculator basis for calculating the necessary parameters. Under the flowsheeting options block, a calculator block could be implemented. By selecting it, a mathematical model can be implemented. The two input methods to implement this model are Fortran and Microsoft Excel.

As Fortran was a difficult coding method, Microsoft Excel was utilized to obtain results and analyze them from the aspen simulation and given parameters. Aspen offers a method where implementing an excel sheet can act as a “code” to organize and calculate any of the values we wanted. By using excel commands and inserting equations, variables could be solved for given a set of input variables. Similar to the previous case utilizing IDAES, the same values were utilized to try and compare/contrast the two programs to see which is a better fit for the project.

Our import variables, which are the variables that are given and utilized to calculate variables, were the temperature, fuel utilization, resistance and respective pressures. Once these are implemented, export variables can be included to be solved for. These export variables are the efficiency, power, and electric potential of the SOFC. Refer to Appendix C to see the list of import and export variables.

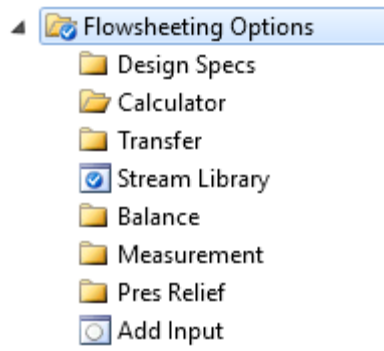


Figure 15: Aspen Plus Flowsheeting Options

4.2.2 Results and Discussion

By utilizing the excel sheet and the Calculator Block within Aspen plus, the program was able to create a number of different situations with varying pressures, temperatures, and mathematical expressions to understand and analyze where the SOFC can be improved and what factors play a part in the performance of the fuel cell. All of these factors impacted the electric potential of the stack. To understand how different pressures can affect the SOFC, three different pressures were taken with the current density and voltage during operation. By increasing pressure slightly, the operating voltage was able to be slightly increased. Voltage gradients were very similar with each other until when the SOFC reached a current density of .6 A/cm². When the SOFC hits this value, voltage drop off begins to skyrocket and vary wildly. This is due to the ohmic losses in the voltage drop due to the transfer of electrons and movement of ions through the electrolyte. This can also be represented with the equation of $E = E_{ocv} - IR - (\eta_a - \eta_c)$. Ohmic losses stem from the resistance of the electrolyte and the electrodes. With a higher pressure, starting operating voltage is higher compared to its counterparts and the overall ohmic voltage loss is smaller with higher pressures. As previously mentioned, the Nernst voltage potential is incredibly important in the assessment of the SOFC's operating standards. By utilizing the equation, it was found that the Nernst potential of the SOFC increased with decreasing operating temperature, which is a positive outlook to want. However, with this

increase Nernst potential comes with an increase in electrochemical losses. Despite the increase in Nernst potential, electrochemical losses outweighed it, which would lead to a decreased power production and cell efficiency as it relates to higher heat waste.

Voltage(V) vs. Current Density (A/cm²) @ 1 Atm

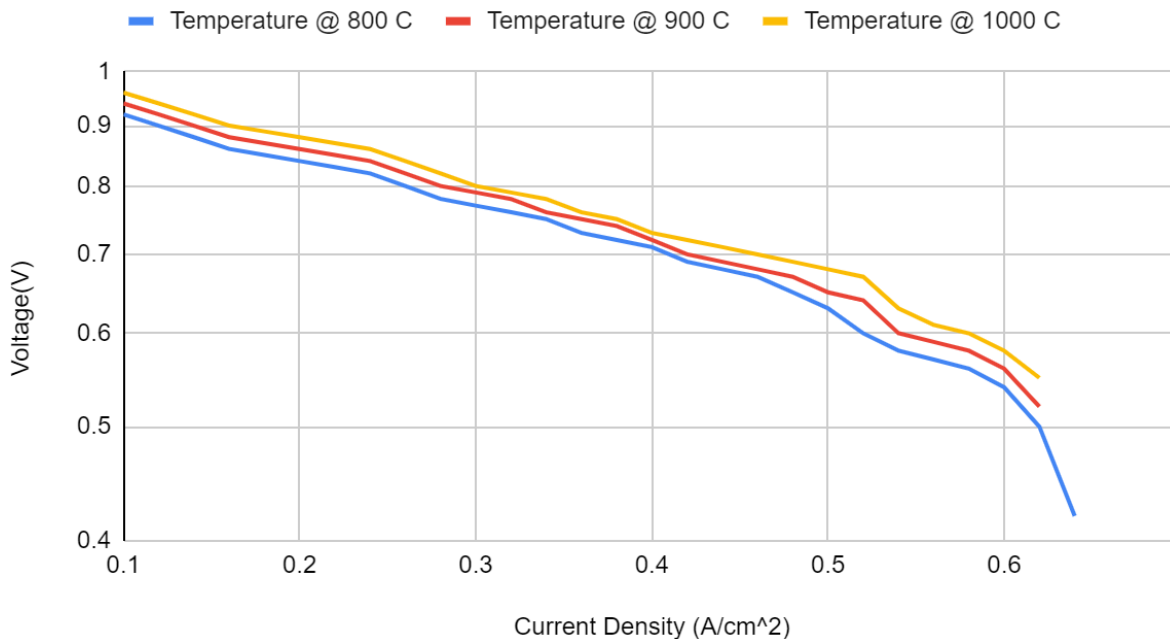


Figure 16: Polarization Curve at constant pressure (1 atm) and varying temperatures.

A similar trend can also be seen with the SOFC system with a constant pressure parameter and varying temperatures. In this scenario, by changing the overall temperature of the SOFC, performance can be manipulated. It was also found that with increasing temperature, many of these polarization losses are minimized. Temperature is a variable that can be easily changed for the SOFC. When looking at activation polarization, by lowering the point it is able to polarize, it leads to a stronger range in power density for the stack. In essence, by increasing the temperature, activation polarization can be reduced, improving efficiency of the SOFC. When the temperature is on the lower side, the curve leading to the polarization will be slightly larger, leading to increased time in processing. This is important as the polarization curve helps to determine the optical fuel cell output voltage given a current density loading. Looking at the figure below, the SOFC when it is working with an operating temperature of 1000 degrees celsius has the highest output voltage. All three temperature variations followed a very similar

linear trend, until the SOFC reached an operating current density of .6 A/cm², identical to IDAES' outputs.

Voltage(V) vs. Current Density (A/cm²) @ 1 Atm

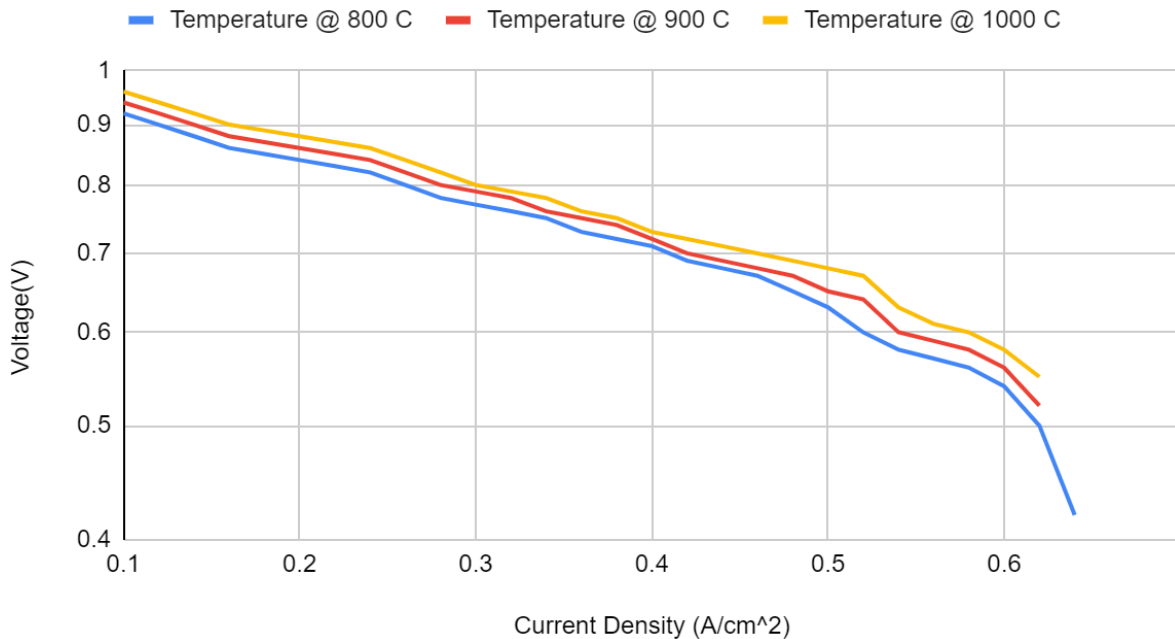


Figure 17: Polarization Curve at constant temperature (1000C) and varying pressures

4.3 Comparison of Modeling Techniques

4.3.1 Benefits of the Software Packages

IDAES has many benefits and useful features when it comes to modeling processes as it provides an innovative approach for the design and optimization of these processes by integrating the Pyomo library. IDAES allows to quickly and easily calculate the output of an SOFC when given a set of initial parameters since it is equation oriented and based in Python. By building off of Python's environment, users can get access to Python's abilities in terms of data visualization and management. It is also flexible in the fact that it has access to Python's wide range of libraries and has the ability to solve numerous types of equation systems, from linear ordinary differential equations to higher-order partial differential equations. Additionally, the fact that the software is open source means that more resources are available for users to collaborate. Due to its advanced capabilities, using this software environment will allow the team to model an SOFC from the simplest model to complex hybrid systems.

Similarly, Aspen Plus' software has an existing database of species and components along with their pure/binary regressed parameters. In other words, properties and their values for both heterogeneous and homogeneous species are already inputted within the simulation software. This reduces the amount of data input needed to run the simulation and reduces the time spent in setting it up as well. Aspen modeling allows for the simulation to avoid overdesigning, number of parts, energy costs, product quality, and eventually achieve higher throughputs.

The proper usage of Aspen plus provides companies with distinct economic benefits throughout their manufacturing processes. The steady-state process simulation power it provides allows for strong modeling power and ease. This comes from the high flexibility it contains involving different process configurations. Typically, R&D groups would benefit the most from this program as it helps to evaluate the feasibility and key operating variables.

4.3.2 Limitations of the Software Packages

While IDAES has many benefits for modeling complex systems such as SOFCs, there are some drawbacks that may limit the software's capabilities. IDAES lacks any user interface, making it difficult for users to interact with the program. All interactions are done via text-based programming. This presents an obstacle for users not familiar with Python. Additionally, a major hindrance in using IDAES is its tedious installation process. It requires access to Github and is installed through a command prompt in several steps, which may fail at any point. As there is no install wizard, it may be difficult for some users to access this software if they are not familiar with programming and command-line interaction. Additionally, IDAES is a relatively new software package released in 2020, so there is incomplete and missing documentation on certain modeling properties that may deem useful for certain models. There is also a lack of example code in the documentation that would be helpful to reference when modeling. Due to the lack of documentation and examples, this would cause difficulty in modeling the SOFC as it would need to be done without prior literature or documentation as a reference. Despite these limitations, IDAES is a strong software package that will create the possibility of modeling such complex models.

Aspen Plus and its components are great simulation tools that come with a few caveats for first time users. Many of these limitations stem from the cost of the program and the exclusivity of it. Obtaining a license requires some work in attaining as communication with

AspenTech needs to be established. Despite the company offering seminars, workshops, and training to learn more about the program, assuming the price of each is covered. To understand the program and its underpinnings, individuals are mostly on their own to learn more. This can revolve around different processes, unit operations, materials such as polymers and electrolytes, and other components. With much of the model being free standing, it is up to the user to ensure assumptions are stated and with different types of modeling, different limitations are led. Different thermodynamic models and conditions will also have an impact on the limitations of the model (Mutlu & Zeng, 2020). When the program is combined with another type of software and coding such as MATLAB, different models and their conditions can be calculated. As Aspen is a chemical simulation software, its basic models don't include electrochemical reactions, which leads to the incorporation of coding models. MATLAB and Fortran are the two types of codes that can be utilized within the application. MATLAB is a very strong coding language with a high ease of accessibility, however Fortran is more outdated and outmoded. The lack of expressiveness and ease of programming is always compared to today's other programming languages. With an awkward source format, lack of dynamic and safe storage, lack of parallelism for vectors, and a lack of numeric portability, MATLAB offers answers to all of Fortran's shortcomings (Drawbacks of FORTRAN77, n.d.).

5. Conclusions and Recommendation

5.1 Conclusions

The group focuses on utilizing two simulation softwares to effectively fabricate, analyze, and compare the thermodynamic properties and efficiency of the SOFC. IDAES focused on the sheer calculations behind properties through the use of coding, while Aspen Plus was much better suited to determine chemical properties and constants for SOFC operation. Values were automatically calculated, which made it much simpler to analyze. While with IDAES, it was perfect to create specific case studies on the SOFC and its operation. It could implement environmental conditions for the SOFC such as operating temperature, pressure, and fuel utilization, and was able to visualize these results onto a graph. Both in tandem helped to create a big picture about both the electrochemical processes and mechanical processes that occurred within the SOFC.

Aspen plus is a very strong and versatile chemical engineering simulation program that strives in any process with multiple models. Despite the license being incredibly expensive along with a steep learning curve, once the user learns the ins and outs of the programs, this program is viewed to be a stronger asset compared to its IDAES counterpart. This is due to the in-depth analysis of every flow inlet and outlet within the setup. Aspen Plus is able to obtain the properties of any chemical substance at any point of the simulation, whether it is the inlet/outlet flow of any block or at the end of the simulation. Properties can be easily found and listed with every flow being recorded and analyzed. This allows for such tedious work to be simplified as the program solves for properties without any equations. This is much stronger compared to IDAES, but there are some flaws within the program due to the nature of the project. Since the project also includes electrochemical properties such as voltage, current density, resistance, and other different properties, Aspen is not necessarily able to calculate and work with these properties. This is due to the program revolving around chemical models and not electrical ones. However, IDAES has a better method to obtain values of properties that cannot be done with the program. This is due to IDAES having an overall better coding platform, as opposed to Aspen's coding software of Fortran. Fortran is severely outdated and lacks a lot of what IDAES coding platform offers which is flexibility and parallelity. As such, this report utilized the excel sheet path to utilize the calculator blocks. This was much easier to create equations and solve for

properties, values, and create the graphs that are associated with them. IDAES in this instance is seen to be the stronger counterpart as the coding behind it comes with easy accessibility and much simpler coding.

Aspen Plus and IDAES are both strong simulation and computational tools. Each has their strong suits that heavily contribute to most of the findings and analysis done within this project.. IDAES offers a lot of freedom and variability. This is due to the extent its coding software is able to reach out and produce. The use of Jupyter Notebooks allows the IDAES platform to easily be edited, with the ability to only run small chunks of code at a time, saving valuable time and effort. Since IDAES uses Python, a very simple and widely accessible programming language, as its method of interaction, it is fairly accessible to anyone familiar with the language. However, due to IDAES being quite a new software, there is little literature regarding its use in modeling SOFCs when compared to Aspen, a software that has been in use for much longer. As a result, we had to modify an existing model for a different kind of simulation to fit our needs, which presented some challenges.

Preliminary research implied that with higher operating temperatures, increased pressures, and a larger fuel utilization, SOFC operation and performance would be maximized. For the most part, this was the case, however, there were a few situations where results were not what we were expecting. As a result of our simulations, the different platforms we used provided us two similar datasets that supplemented polarization curves. The IDAES simulation observed two datasets, constant pressure conditions at various temperatures and constant temperature conditions at various temperatures. When plotted at each temperature and compared, the curves drop at low current densities, more so at increased operating temperatures (between 800C and 1000C). The methodology and its studies were also followed utilizing the Aspen simulation software. Similarly, the Aspen simulation found that around a current density of .6 A/cm², the curve began to have sharp drops. The Aspen simulation also shows that lower temperatures produce larger curves leading up to polarization. In addition, the numerous graphs that our IDAES simulation produced show that while increased inlet fuel pressure improves efficiency, increased operating temperature has little to no effect on SOFC efficiency.

5.2 Recommendations

After comparing the two simulations and what they can offer, the influence of inlet gas composition, temperature, and pressure were the three main aspects that drastically affected the SOFC and its performance. Different instances of operating conditions can be combined to ensure the maximum efficiency it can attain. As it is a fuel cell, it benefits from utilizing pure oxygen as opposed to air as it helps to reduce the operating voltage. By reducing voltage, it leads to smaller voltage and diffusion losses and a higher operating current density. By also including a higher concentration of hydrogen, it improves fuel cell operation by increasing the Nernst voltage while reducing diffusion losses at the electrode. Regarding temperature, an increasing temperature is needed for a fuel cell performance however, this isn't always the case as low current densities paired with low temperatures help offer better performance by minimizing losses. However, this isn't desired as a higher current density has been previously mentioned to be more beneficial. Overall, in almost all scenarios except when dealing with low current densities, a higher temperature is preferred. Lastly, pressure plays a crucial part in the performance of the SOFC as it relates to the partial pressures utilized in previous equations. The Nernst voltage increases with pressure, while losses through diffusion decrease, given that the fuel cell surpasses a certain current density.

6. References

- American Society of Mechanical Engineers [ASME] , (2012). Society Policy. ASME. Retrieved February 17, 2022, from <https://www.asme.org/wwwasmeorg/media/resourcefiles/aboutasme/get%20involved/advocacy/policy-publications/p-15-7-ethics.pdf>
- Baldi, F., Wang, L., Pérez-Fortes, M., & Maréchal, F. (2019). A Cogeneration System Based on Solid Oxide and Proton Exchange Membrane Fuel Cells With Hybrid Storage for Off-Grid Applications . *Frontiers in Energy Research* , 6.
<https://doi.org/10.3389/fenrg.2018.00139>
- Boundless. (n.d.). *Boundless physics*. Lumen. Retrieved April 26, 2022, from <https://courses.lumenlearning.com/boundless-physics/chapter/the-second-law-of-thermodynamics/>
- Cifuentes, A., Husar, A., Roda, V., Morales, M., Bernadet, L., Torrell, M., & Serra, M. (n.d.). *Modeling of Solid Oxide Electrolyzer and hydrogen leak estimation*. 3.
Design and Optimize Chemical Processes with Aspen Plus. (n.d.). Retrieved April 26, 2022, from <https://www.aspentech.com/en/products/pages/aspen-plusrt>
- Download Open-Source IDAES PSE Framework – IDAES*. (n.d.). Retrieved December 21, 2021, from <https://idaes.org/download-open-source-idaes-pse-framework/>
- Drawbacks of FORTRAN 77*. (n.d.). Retrieved April 26, 2022, from <https://www.mrao.cam.ac.uk/~pa/f90Notes/HTMLNotesnode6.html>
- Energy education: Concepts and practice [UWSP], (n.d.). Retrieved April 16, 2022, <https://www3.uwsp.edu/cnr-ap/KEEP/nres633/Pages/Unit2/Section-B-Energy-Transfer.aspx>

Entropy and the Second Law of Thermodynamics. (2021, November 7).

<https://chem.libretexts.org/@go/page/21905>

Entropy Rules. (2022, April 10). Simon Fraser University.

<https://chem.libretexts.org/@go/page/3595>

Fan, L., Tu, Z., & Chan, S. H. (2021). Recent development of hydrogen and Fuel Cell Technologies: A Review. *Energy Reports*, 7, 8421–8446.

<https://doi.org/10.1016/j.egy.2021.08.003>

Fehribach, J.D., & O'Hayre, R. (2009). Triple Phase Boundaries in Solid-Oxide Cathodes. *SIAM Journal on Applied Mathematics*, 70(2), 510–530. <http://www.jstor.org/stable/27798788>

Figure 1. Polarization curves validation of a small-SIZED single rSOC... (n.d.). ResearchGate.

Retrieved April 26, 2022, from

https://www.researchgate.net/figure/Polarization-curves-validation-of-a-small-SIZED-single-rSOC-though-the-0D-modeling_fig1_344378960

Figure 7. Optimal efficiency of the overall system and the optimal SOFC... (n.d.). ResearchGate.

Retrieved December 21, 2021, from

https://www.researchgate.net/figure/Optimal-efficiency-of-the-overall-system-and-the-optimal-SOFC-operating-temperatures-as-a_fig4_265291968

Fuel Cell Fundamentals | Wiley Online Books. (n.d.). Retrieved December 21, 2021, from

<https://onlinelibrary.wiley.com/doi/book/10.1002/9781119191766>

Hauck, M., Herrmann, S., & Spliethoff, H. (2017). Simulation of a reversible SOFC with Aspen Plus. *International Journal of Hydrogen Energy*, 42(15), 10329–10340.

<https://doi.org/10.1016/j.ijhydene.2017.01.189>

Hussain, S., & Yangping, L. (2020). Review of solid oxide fuel cell materials: Cathode, anode, and electrolyte. *Energy Transitions*, 4(2), 113–126.

<https://doi.org/10.1007/s41825-020-00029-8>

IDAES – Institute for the Design of Advanced Energy Systems. (n.d.). Retrieved April 26, 2022, from <https://idaes.org/>

Khan Academy. (n.d.). The laws of thermodynamics (article). Khan Academy. Retrieved April 26, 2022, from <https://www.khanacademy.org/science/ap-biology/cellular-energetics/cellular-energy/a/the-laws-of-thermodynamics>

Kosaksri, K., Jongjitjaroen, M., Srinophakun, T., Fowler, M. W., & Croiset, E. (n.d.). *Optimal Operation of Tubular Solid Oxide Fuel Cell Based on*. 13.

Lang, M., Bohn, C., Henke, M., Schiller, G., Willich, C., & Hauler, F. (2017). Understanding the Current-Voltage Behavior of High Temperature Solid Oxide Fuel Cell Stacks. *Journal of The Electrochemical Society*, 164(13), F1460. <https://doi.org/10.1149/2.1541713jes>

Modeling solid oxide fuel cells. (2008). Fuel Cells and Hydrogen Energy. <https://doi.org/10.1007/978-1-4020-6995-6>

Moran, M. J., Shapiro, H. N., Boettner, D. D., & Bailey, M. B. (2014). *Fundamentals of Engineering Thermodynamics* (Eighth). Wiley.

Mutlu, Ö. Ç., & Zeng, T. (2020). Challenges and Opportunities of Modeling Biomass Gasification in Aspen Plus: A Review. *Chemical Engineering & Technology*, 43(9), 1674–1689. <https://doi.org/10.1002/ceat.202000068>

Nafees, A., & Abdul Rasid, R. (2019). Study of natural gas powered solid oxide fuel cell simulation and modeling. *IOP Conference Series: Materials Science and Engineering*, 702(1), 012017. <https://doi.org/10.1088/1757-899X/702/1/012017>

- Rasidi, R. A. (2019, November 1). Study of Natural Gas Powered Solid Oxide Fuel Cell Simulation & Modeling. IOP Conference Series: Materials Science and Engineering. Retrieved April 26, 2022, from <https://iopscience.iop.org/article/10.1088/1757-899X/702/1/012017>
- Rokni, M. (2013). Thermodynamic analysis of SOFC (solid oxide fuel cell)–Stirling hybrid plants using alternative fuels. *Energy*, *61*, 87–97. <https://doi.org/10.1016/j.energy.2013.06.001>
- Sarikaya, A., Petrovsky, V., & Dogan, F. (2012). Effect of the anode microstructure on the enhanced performance of solid oxide fuel cells. *International Journal of Hydrogen Energy*, *37*(15), 11370–11377. <https://doi.org/10.1016/j.ijhydene.2012.05.007>
- Schöffner, S. I., Klein, S. A., Aravind, P. V., & Pecnik, R. (2021). A solid oxide fuel cell-supercritical carbon dioxide Brayton cycle hybrid system. *Applied Energy*, *283*, 115748. <https://doi.org/10.1016/j.apenergy.2020.115748>
- Simulation of a reversible SOFC with Aspen Plus—ScienceDirect*. (n.d.). Retrieved April 26, 2022, from <https://www.sciencedirect.com/science/article/abs/pii/S0360319917303579>
- SOFC OPERATING PRINCIPLE*. (n.d.). Netl.Doe.Gov. Retrieved April 27, 2022, from <https://netl.doe.gov/carbon-management/sofc/operating-principle>
- Solid oxide cells, Cerpotech*. (n.d.). Retrieved December 21, 2021, from <https://www.cerpotech.com/applications/solid-oxide-cells>
- Solid oxide fuel cell. (2022). In *Wikipedia*. https://en.wikipedia.org/w/index.php?title=Solid_oxide_fuel_cell&oldid=1077056548

Solid Oxide Fuel Cells. (n.d.). Retrieved December 21, 2021, from

<https://mypages.iit.edu/~smart/garrear/fuelcells.htm>

Solid Oxide Fuel Cells Electrolyte—An overview | *ScienceDirect Topics*. (n.d.). Retrieved April

26, 2022, from

<https://www.sciencedirect.com/topics/engineering/solid-oxide-fuel-cells-electrolyte>

Solid oxide fuel cells (SOFCs): A review of an environmentally clean and efficient source of

energy—ScienceDirect. (n.d.). Retrieved April 26, 2022, from

<https://www.sciencedirect.com/science/article/abs/pii/S136403210200014X?via%3Dihub>

Spiegel, D. C. (n.d.). *Polarization Curves*. Retrieved October 20, 2021, from

<https://www.fuelcellstore.com/blog-section/polarization-curves>

Stambouli, A. B., & Traversa, E. (2002, June 18). *Solid oxide fuel cells (SOFCs): A review*

of an environmentally clean and efficient source of energy. *Renewable and Sustainable*

Energy Reviews. Retrieved March 4, 2022, from

<https://www.sciencedirect.com/science/article/abs/pii/S136403210200014X>

Types of fuel cells. *Energy.gov*. (n.d.). Retrieved April 26, 2022, from

<https://www.energy.gov/eere/fuelcells/types-fuel-cells>

Understanding the Current-Voltage Behavior of High Temperature Solid Oxide Fuel Cell

Stacks—IOPscience. (n.d.). Retrieved April 26, 2022, from

<https://iopscience.iop.org/article/10.1149/2.1541713jes>

Wang, D., Bao, J., Xu, Z., & (“KaiChi”) He, Q. (2021). *Machine learning for Natural Gas to*

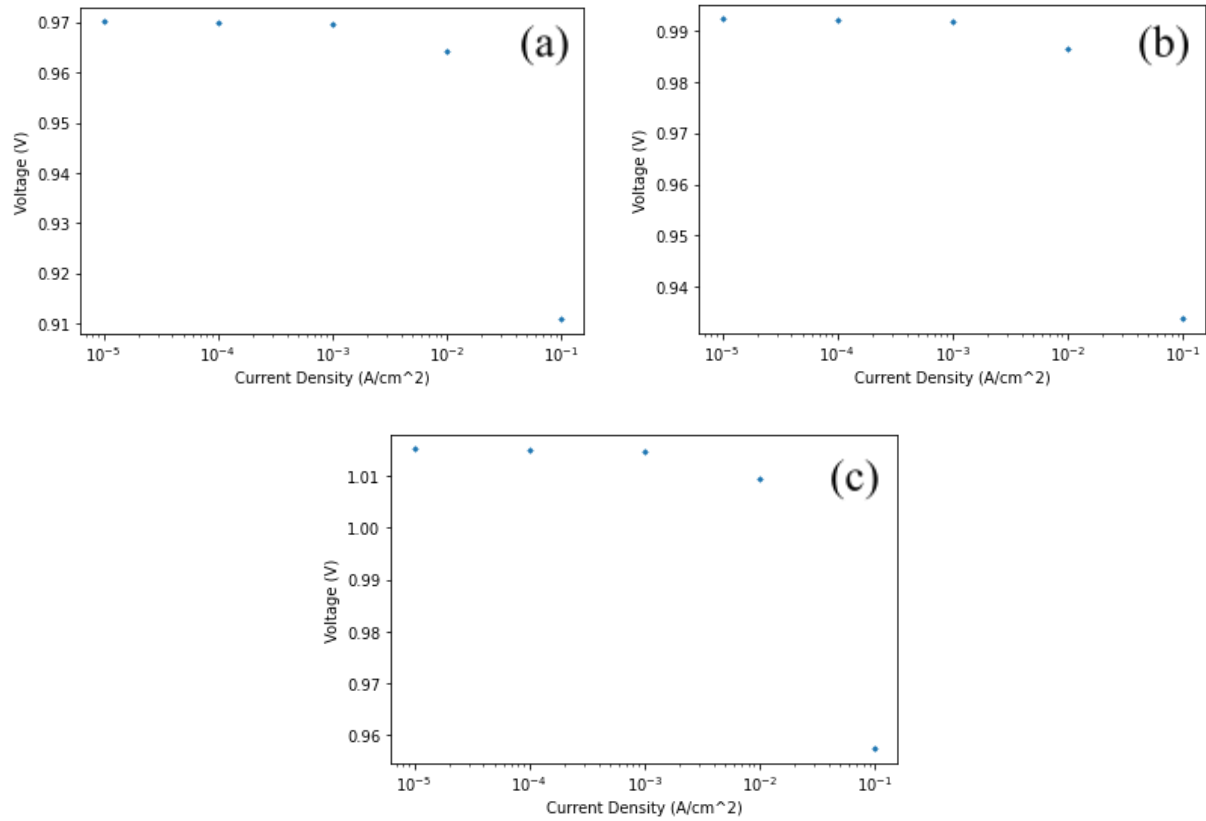
Electric Power System Design [Other].

<https://doi.org/10.26226/morressier.612f6739bc981037241009bb>

7. Appendices

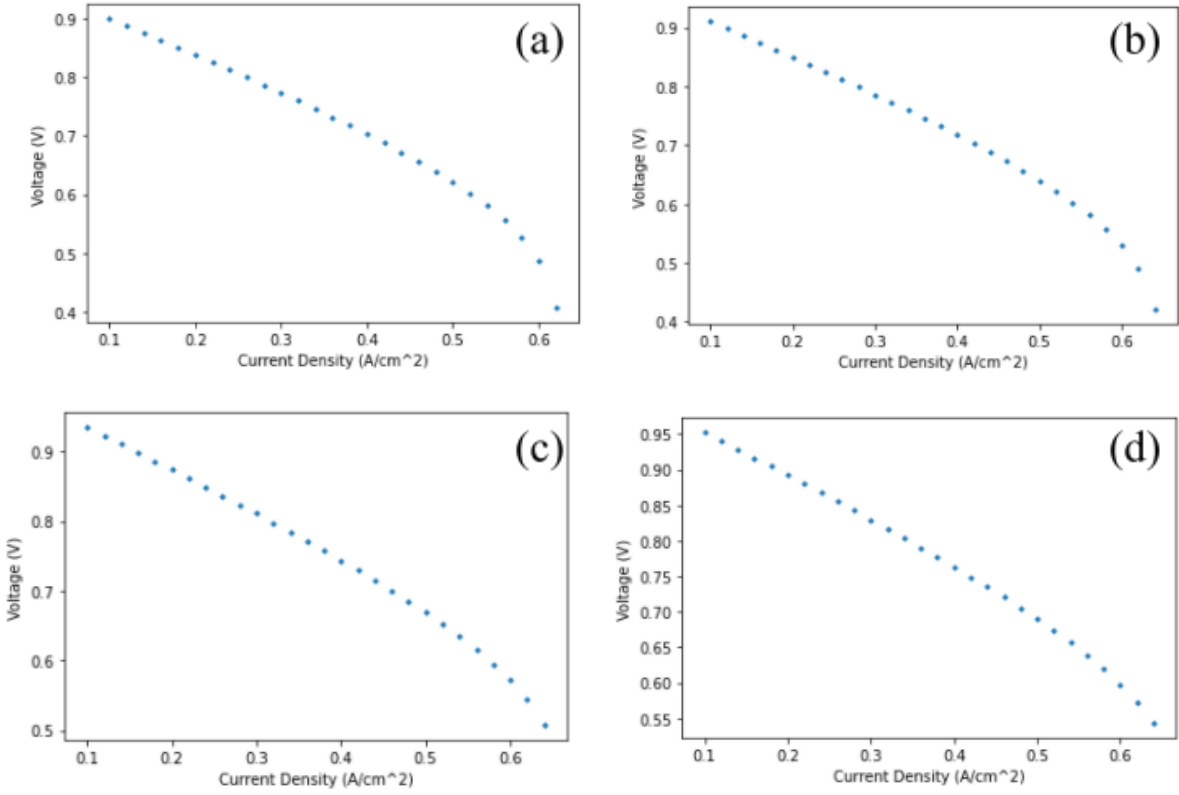
Appendix A

IDAES Logarithmic Polarization Curves for Low Current Densities at Various Temperatures (a) 800C, (b) 900C, and (c) 1000C and Constant Pressure (1 atm)



Appendix B

IDAES Polarization Curves for Various Pressures (a) 0.5 atm, (b) 1 atm, (c) 2 atm and (d) 3 atm at Constant Temperature (1000C)



Appendix C.1

Aspen Plus Flowsheet Flow Properties Page 1

	Units	A3	A4-FUEL	A5-A4-O	A6	F6	F7-FUEL	F8-RXNPR	F9	O2-AN	O2-CAT	
Description												
From			SOFC-CAT	HX-CAT-1	HX-CAT-2		HEATER1	SOFC-AN	HEATER2		HX-CAT-1	
To		SOFC-CAT	HX-CAT-1	HX-CAT-2		HEATER1	SOFC-AN	HEATER2		SOFC-AN		
Stream Class		CONVEN										
Maximum Relative Error												
Cost Flow	\$/hr											
MIXED Substream												
Phase		Vapor Phase										
Temperature	C	799.85	848	848	848	848	848	848	848	848	848	
Pressure	bar	0.506625	1	1	1	1	1	1	1	1	1	
Molar Vapor Fraction		1	1	1	1	1	1	1	1	1	1	
Molar Liquid Fraction		0	0	0	0	0	0	0	0	0	0	
Molar Solid Fraction		0	0	0	0	0	0	0	0	0	0	
Mass Vapor Fraction		1	1	1	1	1	1	1	1	1	1	
Mass Liquid Fraction		0	0	0	0	0	0	0	0	0	0	
Mass Solid Fraction		0	0	0	0	0	0	0	0	0	0	
Molar Enthalpy	cal/mol	6031.74	6437.55	6437.55	6437.55	5818.32	5818.32	5994	5994	6437.55	6437.55	
Mass Enthalpy	cal/gm	188.499	201.181	201.181	201.181	2886.24	2886.24	187.961	187.961	201.181	201.181	
Molar Entropy	cal/mol-K	11.1413	10.1609	10.1609	10.1609	9.34275	9.34275	10.1805	10.1805	10.1609	10.1609	
Mass Entropy	cal/gm-K	0.34818	0.317541	0.317541	0.317541	4.63458	4.63458	0.319242	0.319242	0.317541	0.317541	
Molar Density	mol/cc	5.67884e-06	1.07278e-05									
Mass Density	gm/cc	0.000181716	0.000343275	0.000343275	0.000343275	2.16259e-05	2.16259e-05	0.000342103	0.000342103	0.000343275	0.000343275	
Enthalpy Flow	cal/sec	3.29232	3.51383	1.75691	1.75691	1.80271	1.80271	237.692	237.692	254.283	1.75691	
Average MW		31.9988	31.9988	31.9988	31.9988	2.01588	2.01588	31.8895	31.8895	31.9988	31.9988	
✦ Mole Flows	kmol/hr	0.001965	0.001965	0.0009825	0.0009825	0.0011154	0.0011154	0.142758	0.142758	0.1422	0.0009825	
✦ Mole Fractions												
✦ Mass Flows	kg/hr	0.0628776	0.0628776	0.0314388	0.0314388	0.00224851	0.00224851	4.55248	4.55248	4.55023	0.0314388	
✦ Mass Fractions												
Volume Flow	l/min	5.76702	3.05283	1.52641	1.52641	1.73289	1.73289	221.789	221.789	220.922	1.52641	

Appendix C.2

Aspen Plus Flowsheet Flow Properties Page 2

	Units	A3	A4-FUEL	A5-A4-O	A6	F6	F7-FUEL	F8-RXNPR	F9	O2-AN	O2-CAT	
WATER								5013.68	5013.68			
- K-Values, vapor/Liquid 2												
OXYGE-01												
HYDRO-01												
WATER												
- Heat capacity, constant volume												
OXYGE-01	cal/mol-K	6.39878	6.44534	6.44534	6.44534			6.44534	6.44534	6.44534	6.44534	
HYDRO-01	cal/mol-K					5.32708	5.32708	5.32708	5.32708			
WATER	cal/mol-K							8.21447	8.21447			
Mass flow of hydrogen atoms	kg/hr	0	0	0	0	0.00224842	0.00224842	0.00224842	0.00224842	0	0	
Mass flow of oxygen atoms	kg/hr	0.0628776	0.0628776	0.0314388	0.0314388	0	0	4.55023	4.55023	4.55023	0.0314388	
Mass fraction of hydrogen atoms		0	0	0	0	0.99996	0.99996	0.00049389	0.00049389	0	0	
Mass fraction of oxygen atoms		1	1	1	1	0	0	0.999506	0.999506	1	1	
Mole flow of hydrogen atoms	kmol/hr	0	0	0	0	0.0022308	0.0022308	0.0022308	0.0022308	0	0	
Mole flow of oxygen atoms	kmol/hr	0.00393	0.00393	0.001965	0.001965	0	0	0.2844	0.2844	0.2844	0.001965	
Mole fraction of oxygen atoms		1	1	1	1	0	0	0.992217	0.992217	1	1	
Mole fraction of hydrogen atoms		0	0	0	0	1	1	0.00778283	0.00778283	0	0	
Gibbs energy departure, mixture	cal/mol	-1476.97	-29.3064	-29.3064	-29.3064	-29.3064	-29.3064	-29.3064	-29.3064	-29.3064	-29.3064	
Enthalpy departure, mixture	cal/mol	0	0	0	0	0	0	0	0	0	0	
Entropy departure, mixture	cal/mol-K	1.37648	0.0261396	0.0261396	0.0261396	0.0261396	0.0261396	0.0261396	0.0261396	0.0261396	0.0261396	
Gibbs energy, mixture	cal/mol	-5922.91	-4954.39	-4954.39	-4954.39	-4656.3	-4656.3	-5419.84	-5419.84	-4954.39	-4954.39	
Enthalpy, mixture	cal/mol	6031.74	6437.55	6437.55	6437.55	5818.32	5818.32	5994	5994	6437.55	6437.55	
Internal energy, mixture	cal/mol	3900.93	4211.12	4211.12	4211.12	3591.89	3591.89	3767.57	3767.57	4211.12	4211.12	
Pressure	bar	0.506625	1	1	1	1	1	1	1	1	1	
Critical pressure, mixture	bar	50.43	50.43	50.43	50.43	13.13	13.13	51.7599	51.7599	50.43	50.43	
Density, mixture	mol/cc	5.67884e-06	1.07278e-05									
- K-values, vapor/liquid												
OXYGE-01		1	1	1	1			6950.88	6950.88	1	1	
HYDRO-01						1	1	14425.3	14425.3			

Appendix C.3

Aspen Plus Flowsheet Flow Properties Page 3

	Units	A3	A4-FUJEL	A5-A4-O	A6	F6	F7-FUJEL	F8-RXNPR	F9	O2-AN	O2-CAT
- Vapor Phase											
Molar Enthalpy	cal/mol	6031.74	6437.55	6437.55	6437.55	5818.32	5818.32	5994	5994	6437.55	6437.55
Mass Enthalpy	cal/gm	188.499	201.181	201.181	201.181	2886.24	2886.24	187.961	187.961	201.181	201.181
Molar Entropy	cal/mol-K	11.1413	10.1609	10.1609	10.1609	9.34275	9.34275	10.1805	10.1805	10.1609	10.1609
Mass Entropy	cal/gm-K	0.34818	0.317541	0.317541	0.317541	4.63458	4.63458	0.319242	0.319242	0.317541	0.317541
Molar Density	mol/cc	5.67884e-06	1.07278e-05	1.07278e-05	1.07278e-05	1.07278e-05	1.07278e-05	1.07278e-05	1.07278e-05	1.07278e-05	1.07278e-05
Mass Density	gm/cc	0.000181716	0.000343275	0.000343275	0.000343275	2.16259e-05	2.16259e-05	0.000342103	0.000342103	0.000343275	0.000343275
Enthalpy Flow	cal/sec	3.29232	3.51383	1.75691	1.75691	1.80271	1.80271	237.692	237.692	254.283	1.75691
Average MW		31.9988	31.9988	31.9988	31.9988	2.01588	2.01588	31.8895	31.8895	31.9988	31.9988
- Mole Flows											
	kmol/hr	0.001965	0.001965	0.0009825	0.0009825	0.0011154	0.0011154	0.142758	0.142758	0.1422	0.0009825
OXYGE-01	kmol/hr	0.001965	0.001965	0.0009825	0.0009825	0	0	0.141642	0.141642	0.1422	0.0009825
HYDRO-01	kmol/hr	0	0	0	0	0.0011154	0.0011154	2.48063e-12	2.48063e-12	0	0
WATER	kmol/hr	0	0	0	0	0	0	0.0011154	0.0011154	0	0
- Mole Fractions											
OXYGE-01		1	1	1	1	0	0	0.992187	0.992187	1	1
HYDRO-01		0	0	0	0	1	1	1.73765e-11	1.73765e-11	0	0
WATER		0	0	0	0	0	0	0.00781324	0.00781324	0	0
- Mass Flows											
	kg/hr	0.0628776	0.0628776	0.0314388	0.0314388	0.00224851	0.00224851	4.55248	4.55248	4.55023	0.0314388
OXYGE-01	kg/hr	0.0628776	0.0628776	0.0314388	0.0314388	0	0	4.53238	4.53238	4.55023	0.0314388
HYDRO-01	kg/hr	0	0	0	0	0.00224851	0.00224851	5.00065e-12	5.00065e-12	0	0
WATER	kg/hr	0	0	0	0	0	0	0.0200942	0.0200942	0	0
- Mass Fractions											
OXYGE-01		1	1	1	1	0	0	0.995586	0.995586	1	1
HYDRO-01		0	0	0	0	1	1	1.09845e-12	1.09845e-12	0	0
WATER		0	0	0	0	0	0	0.00441391	0.00441391	0	0
Volume Flow	l/min	5.76702	3.05283	1.52641	1.52641	1.73289	1.73289	221.789	221.789	220.922	1.52641
Gibbs energy departure, mixture	cal/mol	-1476.97	-29.3064	-29.3064	-29.3064	-29.3064	-29.3064	-29.3064	-29.3064	-29.3064	-29.3064
Gibbs energy, mixture	cal/mol	-5922.91	-4954.39	-4954.39	-4954.39	-4656.3	-4656.3	-5419.04	-5419.04	-4954.39	-4954.39
- Ratio of C₀/C₁											

Appendix C.4

Aspen Plus Flowsheet Flow Properties Page 4

	Units	A3	A4-FUEL	A5-A4-O	A6	F6	F7-FUEL	F8-RXNPR	F9	O2-AN	O2-CAT	
- Ratio of Cp/Cv												
OXYGE-01		1.30979	1.30756	1.30756	1.30756			1.30756	1.30756	1.30756	1.30756	
HYDRO-01						1.37191	1.37191	1.37191	1.37191			
WATER								1.24147	1.24147			
- Heat capacity pure component												
OXYGE-01	cal/mol-K	8.40448	8.45104	8.45104	8.45104			8.45104	8.45104	8.45104	8.45104	
HYDRO-01	cal/mol-K					7.33279	7.33279	7.33279	7.33279			
WATER	cal/mol-K							10.2202	10.2202			
- Partial pressure												
OXYGE-01	bar	0.506625	1	1	1			0.992187	0.992187	1	1	
HYDRO-01	bar					1	1	1.73765e-11	1.73765e-11			
WATER	bar							0.00781324	0.00781324			
- Mole fraction												
OXYGE-01		1	1	1	1	0	0	0.992187	0.992187	1	1	
HYDRO-01		0	0	0	0	1	1	1.73765e-11	1.73765e-11	0	0	
WATER		0	0	0	0	0	0	0.00781324	0.00781324	0	0	
- Mole flow rate												
OXYGE-01	kmol/hr	0.001965	0.001965	0.0009825	0.0009825	0.0011154	0.0011154	0.142758	0.142758	0.1422	0.0009825	
HYDRO-01	kmol/hr	0.001965	0.001965	0.0009825	0.0009825	0.0011154	0.0011154	2.48063e-12	2.48063e-12	0	0	
WATER	kmol/hr	0	0	0	0	0	0	0.0011154	0.0011154	0	0	
- Mass flow rate												
OXYGE-01	kg/hr	0.0628776	0.0628776	0.0314388	0.0314388	0.00224851	0.00224851	4.55248	4.55248	4.55023	0.0314388	
HYDRO-01	kg/hr	0	0	0	0	0.00224851	0.00224851	5.00065e-12	5.00065e-12	0	0	
WATER	kg/hr	0	0	0	0	0	0	0.0200942	0.0200942	0	0	
- Mass fraction												
OXYGE-01		1	1	1	1	0	0	0.995586	0.995586	1	1	
HYDRO-01		0	0	0	0	1	1	1.09845e-12	1.09845e-12	0	0	
WATER		0	0	0	0	0	0	0.00441391	0.00441391	0	0	
- Ideal gas heat capacity pure comp...												

Appendix C.5

Aspen Plus Flowsheet Flow Properties Page 5

	Units	A3	A4-FUEL	A5-A4-O	A6	F6	F7-FUEL	F8-RXNPR	F9	O2-AN	O2-CAT	
- Gibbs energy departure, pure co...												
OXYGE-01	ca/mol	-1476.97	-29.3064	-29.3064	-29.3064			-29.3064	-29.3064	-29.3064	-29.3064	
HYDRO-01	ca/mol					-29.3064	-29.3064	-29.3064	-29.3064			
WATER	ca/mol							-29.3064	-29.3064			
- Heat capacity, constant volume												
OXYGE-01	ca/mol-K	6.41665	6.46321	6.46321	6.46321			6.46321	6.46321	6.46321	6.46321	
HYDRO-01	ca/mol-K					5.34496	5.34496	5.34496	5.34496			
WATER	ca/mol-K							8.23234	8.23234			
- Thermal conductivity, pure compo...												
OXYGE-01	kcal-m/hr-sqm-K	0.0668136	0.0691907	0.0691907	0.0691907			0.0691907	0.0691907	0.0691907	0.0691907	
HYDRO-01	kcal-m/hr-sqm-K					0.422823	0.422823	0.422823	0.422823			
WATER	kcal-m/hr-sqm-K							0.0973872	0.0973872			
Thermal diffusivity	sqcm/sec	3.88825	2.11961	2.11961	2.11961	14.9301	14.9301	2.12243	2.12243	2.11961	2.11961	
Mass flow of hydrogen atoms	kg/hr	0	0	0	0	0.00224842	0.00224842	0.00224842	0.00224842	0	0	
Mass flow of oxygen atoms	kg/hr	0.0628776	0.0628776	0.0314388	0.0314388	0	0	4.55023	4.55023	4.55023	0.0314388	
Mass fraction of hydrogen atoms		0	0	0	0	0.99996	0.99996	0.00049389	0.00049389	0	0	
Mass fraction of oxygen atoms		1	1	1	1	0	0	0.999506	0.999506	1	1	
Mole flow of hydrogen atoms	kmol/hr	0	0	0	0	0.0022308	0.0022308	0.0022308	0.0022308	0	0	
Mole flow of oxygen atoms	kmol/hr	0.00393	0.00393	0.001965	0.001965	0	0	0.2844	0.2844	0.2844	0.001965	
Mole fraction of oxygen atoms		1	1	1	1	0	0	0.992217	0.992217	1	1	
Mole fraction of hydrogen atoms		0	0	0	0	1	1	0.00778283	0.00778283	0	0	
Gibbs energy departure, mixture	ca/mol	-1476.97	-29.3064	-29.3064	-29.3064	-29.3064	-29.3064	-29.3064	-29.3064	-29.3064	-29.3064	
Enthalpy departure, mixture	ca/mol	0	0	0	0	0	0	0	0	0	0	
Entropy departure, mixture	ca/mol-K	1.37648	0.0261396	0.0261396	0.0261396	0.0261396	0.0261396	0.0261396	0.0261396	0.0261396	0.0261396	
Ideal gas Gibbs energy, mixture	ca/mol	-4445.94	-4925.09	-4925.09	-4925.09	-4626.99	-4626.99	-5390.53	-5390.53	-4925.09	-4925.09	
Gibbs energy, mixture	ca/mol	-5922.91	-4954.39	-4954.39	-4954.39	-4656.3	-4656.3	-5419.84	-5419.84	-4954.39	-4954.39	
Ideal gas enthalpy, mixture	ca/mol	6031.74	6437.55	6437.55	6437.55	5818.32	5818.32	5994	5994	6437.55	6437.55	
Enthalpy, mixture	ca/mol	6031.74	6437.55	6437.55	6437.55	5818.32	5818.32	5994	5994	6437.55	6437.55	
Internal energ. mixture	ca/mol	3900.93	4211.12	4211.12	4211.12	3591.89	3591.89	3767.57	3767.57	4211.12	4211.12	

Appendix C.6

Aspen Plus Flowsheet Flow Properties Page 6

	Units	A3	A4-FUEL	A5-A4-O	A6	F6	F7-FUEL	F8-RXNPR	F9	O2-AN	O2-CAT	
Mass fraction of hydrogen atoms		0	0	0	0	0.99996	0.99996	0.00049389	0.00049389	0	0	
Mass fraction of oxygen atoms		1	1	1	1	0	0	0.999506	0.999506	1	1	
Mole flow of hydrogen atoms	kmol/hr	0	0	0	0	0.0022308	0.0022308	0.0022308	0.0022308	0	0	
Mole flow of oxygen atoms	kmol/hr	0.00393	0.00393	0.001965	0.001965	0	0	0.2844	0.2844	0.2844	0.001965	
Mole fraction of oxygen atoms		1	1	1	1	0	0	0.992217	0.992217	1	1	
Mole fraction of hydrogen atoms		0	0	0	0	1	1	0.00778283	0.00778283	0	0	
Gibbs energy departure, mixture	cal/mol	-1476.97	-29.3064	-29.3064	-29.3064	-29.3064	-29.3064	-29.3064	-29.3064	-29.3064	-29.3064	
Enthalpy departure, mixture	cal/mol	0	0	0	0	0	0	0	0	0	0	
Entropy departure, mixture	cal/mol-K	1.37648	0.0261396	0.0261396	0.0261396	0.0261396	0.0261396	0.0261396	0.0261396	0.0261396	0.0261396	
Ideal gas Gibbs energy, mixture	cal/mol	-4445.94	-4925.09	-4925.09	-4925.09	-4626.99	-4626.99	-5390.53	-5390.53	-4925.09	-4925.09	
Gibbs energy, mixture	cal/mol	-5922.91	-4954.39	-4954.39	-4954.39	-4656.3	-4656.3	-5419.84	-5419.84	-4954.39	-4954.39	
Ideal gas enthalpy, mixture	cal/mol	6031.74	6437.55	6437.55	6437.55	5818.32	5818.32	5994	5994	6437.55	6437.55	
Enthalpy, mixture	cal/mol	6031.74	6437.55	6437.55	6437.55	5818.32	5818.32	5994	5994	6437.55	6437.55	
Internal energy, mixture	cal/mol	3900.93	4211.12	4211.12	4211.12	3591.89	3591.89	3767.57	3767.57	4211.12	4211.12	
Critical pressure, mixture	bar	50.43	50.43	50.43	50.43	13.13	13.13	51.7599	51.7599	50.43	50.43	
Density, mixture	mol/cc	5.67884e-06	1.07278e-05									
- Partial pressure												
OXYGE-01	bar	0.506625	1	1	1			0.992187	0.992187	1	1	
HYDRO-01	bar						1	1.73765e-11	1.73765e-11			
WATER	bar							0.00781324	0.00781324			
Thermal conductivity, mixture	kcal-m/hr-sqm-K	0.0668078	0.0691796	0.0691796	0.0691796	0.422808	0.422808	0.0693849	0.0693849	0.0691796	0.0691796	
Thermal diffusivity	sqcm/sec	3.88825	2.11961	2.11961	2.11961	14.9301	14.9301	2.12243	2.12243	2.11961	2.11961	
- Diffusivity, mixture												
OXYGE-01	sqcm/sec	2.92481	2.92481	2.92481	2.92481			2.92481	2.92481	2.92481	2.92481	
HYDRO-01	sqcm/sec					2.92481	2.92481	6.74967	6.74967			
WATER	sqcm/sec							2.92481	2.92481			
+ Thermal conductivity, pure compo...												
<add properties>												

Appendix D

Code for Calculating Actual Voltage of SOFC and Producing Polarization Curve

```
# Constant Values
R = 8.314 # J/K mol
F = 96485 # C/mol
P_ref = 1 # atm reference is 1atm
i_L = 6500 * 0.0001 # A/cm^2 assumed/input
a = 0.05 #Correction constant assumed/input
B = 0.5 # transfer coefficient assumed/input
gam_a = 2.0*10**8 * 0.0001 # A/cm^2
gam_c = 1.5*10**8 * 0.0001 # A/cm^2
e_a = 105000 #J/mol
e_c = 110000 #J/mol

import pytablewriter
from pytablewriter.style import Style
table1 = pytablewriter.MarkdownTableWriter()
table1.table_name = "SOFC Constant Values and Assumptions"
table1.header_list = ["Constant", "Symbol", "Value", "Units"]
table1.value_matrix = [
["Universal Gas Constant", "R", format(R), "J/K mol"],
["Faraday Constant", "F", format(F, ".1f"), "C/mol"],
["Reference Pressure", "P_ref", format(P_ref, ".1f"), "atm"],
["Limiting Current Density", "i_L", format(i_L, ".3f"), "A/cm^2"],
["Limiting Current Density Correction Factor", "a", format(a, ".3f"), "-"],
["Transfer Coefficient", "B", format(B, ".3f"), "-"],
["Pre-exponential Factor: Anode", "gam_a", format(gam_a, ".3f"), "A/cm^2"],
["Pre-exponential Factor: Cathode", "gam_c", format(gam_c, ".3f"), "A/cm^2"],
["Activation Energy: Anode", "e_a", format(e_a, ".3f"), "J/mol"],
["Activation Energy: Cathode", "e_c", format(e_c, ".3f"), "J/mol"]
```

]

table1

Input Parameters

T = 1073 # K

fuelU = 1

H2_p = 0.5 # atm assumed that anolyte is purely H2

O2_p = 0.21 # atm air is 21% O2

H2O_p = 0.5 # atm all anolyte becomes H2O

R_ohm = 0.5 # ohm*cm² assumed/input

inputtable = pytablewriter.MarkdownTableWriter()

inputtable.table_name = "SOFC Input Values"

inputtable.header_list = ["Input", "Symbol", "Value", "Units"]

inputtable.value_matrix = [

["SOFC Operating Temp", "T", format(T, ".1f"), "K"],

["Fuel Utilization", "fuelU", format(fuelU, ".1f"), ""],

["Input Anolyte Pressure", "H2_p", format(H2_p, ".1f"), "atm"],

["Output Anolyte Pressure", "H2O_p", format(H2O_p, ".1f"), "atm"],

["Catholyte Pressure", "O2_p", format(O2_p, ".2f"), "atm"],

["SOFC Resistance", "R_ohm", format(R_ohm, ".2f"), "ohm*cm²"],

]

inputtable

SOFC Constant Values and Assumptions

Constant Symbol Value Units

Universal Gas Constant R 8.314 J/K mol

Faraday Constant F 96485.000 C/mol

Reference Pressure P_ref 1.000 atm

Limiting Current Density i_L 0.650 A/cm²

Limiting Current Density Correction Factor a 0.050 -

Transfer Coefficient B 0.500 -

Pre-exponential Factor: Anode γ_a 20000.000 A/cm²

Pre-exponential Factor: Cathode γ_c 15000.000 A/cm²

Activation Energy: Anode e_a 105000.000 J/mol

Activation Energy: Cathode e_c 110000.000 J/mol

SOFC Input Values

Input Symbol Value Units

SOFC Operating Temp T 1073.00 K

Fuel Utilization fuelU 1.00

Input Anolyte Pressure H2_p 0.50 atm

Nernst Term Calculation for Open Circuit Voltage

```
nernstterm = ((R*T)/(2*F))*np.log((((H2_p/P_ref)*(np.sqrt((O2_p/P_ref)))/(H2O_p/P_ref)))
```

```
print("Nernst Term: " + format(nernstterm, ".2f"))
```

Gibbs Energy Change Calculation

```
Gibb = (-247.4 + (0.0541*T))*1000
```

Open Circuit Voltage Calculation

```
E_rev = ((Gibb/(2*F)) + nernstterm)*-1
```

```
print("Open-Circuit Voltage: " + format(E_rev, ".3f"))
```

Actual Current Density

```
# i_act = i_op + i_I # actual current density
```

```
# i_act = 0.32 # A/cm^2
```

```
# i_act = np.array([0.1, 0.12, 0.14, 0.16, 0.18, 0.2, 0.22, 0.24, 0.26, 0.28, 0.30, 0.32, 0.34, 0.36, 0.38, 0.4, 0.42, 0.44, 0.46, 0.48, 0.50, ])
```

```

i_act = np.arange(0.1, 0.5, 0.02)
#i_act = np.array([0.0001, 0.001, 0.01, 0.1])

# Ohmic Loss Calculation
E_ohm = i_act*R_ohm
print("Ohmic loss: ", E_ohm)

# Concentration Loss Calculation
i_Ladj = i_L*((H2_p/P_ref)**a)
E_conc = ((R*T)/(2*F))*np.log(1-(i_act/i_Ladj))
# print("Concentration loss: " + format(E_conc, ".3f"))
print("Concentration loss: " , E_conc)

# Activation Loss Calculation
# Anode Exchange Current Density
i_0a = gam_a + ((H2_p/P_ref)*(H2O_p/P_ref)*np.exp(e_a/(R*T)))
Input Anolyte Pressure H2_p 0.50 atm
Output Anolyte
Pressure
H2O_p 0.50 atm
Catholyte Pressure O2_p 0.21 atm
SOFC Resistance R_ohm 0.50 ohm*cm^2
Input Symbol Value Units

Nernst Term: -0.04

Open-Circuit Voltage: 1.017

Ohmic loss: [0.05 0.06 0.07 0.08 0.09 0.1 0.11 0.12 0.13 0.14 0.15 0.16 0.17 0.18
0.19 0.2 0.21 0.22 0.23 0.24]

```

```

Concentration loss: [-0.00802021 -0.00980584 -0.01166323 -0.01359838 -0.01561808
-0.0177300
7
-0.01994318 -0.02226759 -0.02471509 -0.02729944 -0.03003686 -0.03294664
-0.03605193 -0.03938093 -0.04296838 -0.04685783 -0.05110481 -0.05578178
-0.06098574 -0.06685068]

```

```

E_activ_a = np.log(i_act/i_0a)*(-(1-B)/B)*((R*T)/F)
# Cathode Exchange Current Density
i_0c = gam_c + (((O2_p/P_ref)**0.25)*np.exp(e_c/(R*T)))
E_activ_c = np.log(i_act/i_0c)*(-(1-B)/B)*((R*T)/F)
E_activ = (E_activ_a - E_activ_c)/2
# print("Activation loss: " + format(E_activ, ".3f"))
print("Activation loss: " , E_activ)

```

```

# Actual SOFC Voltage Calculation
E_act = E_rev - E_ohm + E_conc + E_activ
# print("Actual SOFC Voltage: " + format(E_act, ".3f"))
print("Actual SOFC Voltage: " , E_act)

```

```

x = i_act
y = E_act
plt.scatter(x,y, marker='D', s=5)
plt.xlabel('Current Density (A/cm^2)')
plt.ylabel('Voltage (V)')
plt.title('SOFC Polarization Curve')
plt.show()

```

n_H2react = 1

Current Produced by SOFC stack per mole fuel

$I = 2 * n_H2react * F$

print(I)

$W_netSOFC = E_act * I$

print("Total Power: ", W_netSOFC)

Activation loss: [-0.05401382 -0.05401382 -0.05401382 -0.05401382 -0.05401382 -0.05401382
-0.05401382 -0.05401382 -0.05401382 -0.05401382 -0.05401382 -0.05401382
-0.05401382 -0.05401382 -0.05401382 -0.05401382 -0.05401382 -0.05401382
-0.05401382 -0.05401382]

Actual SOFC Voltage: [0.90528425 0.89349862 0.88164123 0.86970608 0.85768638

0.84557439

0.83336128 0.82103687 0.80858937 0.79600502 0.7832676 0.77035783

0.75725253 0.74392353 0.73033608 0.71644664 0.70219966 0.68752268

0.67231873 0.65645379]

Total Power: [174692.70235634 172418.42834161 170130.30843068 167827.18314041

efficiency = E_act/E_rev

print("SOFC efficiency: ", efficiency)

Total Power: [174692.70235634 172418.42834161 170130.30843068 167827.18314041

165507.74095253 163170.49051336 160813.72617389 158435.48485854

156033.49150517 153605.08923773 151147.14883952 148655.94969703

146127.02069519 143554.92372428 140932.95301442 138252.70768985

135503.46743525 132671.25130217 129737.34465584 126675.88710874]

SOFC efficiency: [0.88987318 0.87828818 0.86663264 0.85490068 0.84308559 0.83117979
0.81917459 0.80705998 0.79482438 0.78245426 0.76993367 0.75724367
0.74436147 0.73125938 0.71790323 0.70425024 0.69024579 0.67581866
0.66087353 0.64527867]

Appendix E

AspenPlus Coding Parameters

Import Variables

$T = 1073 \text{ K}$

$\text{fuelU} = 1$ -> Fuel Utilisation

$\text{H2_p} = 0.5$ # atm assumed that anolyte is purely H2 -> Pressure

$\text{O2_p} = 0.21$ # atm air is 21% O2 -> Pressure

$\text{H2O_p} = 0.5$ # atm all anolyte becomes H2O -> Pressure

$\text{R_ohm} = 0.5$ ohm*cm² -> Resistance

$\text{e_a} = 105000$ J/mol -> Anode Activation Energy

$\text{e_c} = 110000$ J.mol -> Cathode Activation Energy

$F = 96485$ C/Mol -> Faraday Constant

$\text{alpha} = .05$ -> Limiting Current Density Correction Factor

Export Variables

gam_a = Anode Exchange Current Density

gam_c = Cathode Exchange Current Density

i_act = Actual Density

Appendix F

IDAES Installation Instructions

To install *IDAES*, an understanding of computer console commands, *Github*, and forking repositories is required so that the platform is properly installed without installations. The first step is to install *Miniconda3* to install all of the Python packages. *Miniconda3* is a free minimal installer for *conda*, which is an open-source package management system used to find and install packages for Python. After *Miniconda3* is installed, the *IDAES* package needs to be installed via the *Miniconda3* terminal prompt. To do so, a *Github* account is needed and *Git* needs to be installed. In *Github*, the repository for *IDAES* needs to be forked. Then in the *Miniconda3* terminal, the fork needs to be cloned using a set of commands, and an upstream remote must be added. After the fork is cloned, the Python environment for *IDAES* must be created in the terminal prompt, and the *IDAES* requirements and extensions can be installed. Once *IDAES* has been properly installed and the *IDAES* Python environment has been created, programs and models can be launched with the *Jupyter Notebooks* for editing.

Appendix G

AspenPlus Installation Instructions

AspenTech offers a variety of ASPEN programs. Typically, users install the aspenONE engineering package as it includes most of the different variations of ASPEN software, including Aspen Plus, HYSYS, Exchanger Design & Rating, DMC3 Builder, and more. A thing to note is that for any user to obtain this software, a license must be purchased or given through a third party. Once obtaining a license for the product, navigate towards AspenTech's website and download the aspenONE installer. Through this installation, it shall ask for a license to be plugged in. The installer will also ask for the packages to install onto the computer so the user can pick and choose which applications they are seeking. Once installed, the user is able to interface with any of the packages that were selected and simulations may begin to be fabricated.

